Computers and Mathematics with Applications 69 (2015) 852–875

Contents lists available at ScienceDirect

Computers and Mathematics with Applications

journal homepage: www.elsevier.com/locate/camwa

Stability and bifurcation analysis in a delayed reaction–diffusion malware propagation model

Linhe Zhu [a], Hongyong Zhao [a,*], Xiaoming Wang [b]

[a] Department of Mathematics, Nanjing University of Aeronautics and Astronautics, Nanjing 210016, China

[b] School of Computer Science, Shaanxi Normal University, Xi'an 710062, China

ARTICLE INFO

Article history:
Received 22 April 2014
Received in revised form 29 October 2014
Accepted 4 February 2015
Available online 7 March 2015

Keywords:
Wireless malware
Mobile wireless sensor networks
Discrete time delay
Stability
Hopf bifurcation

ABSTRACT

Mobile wireless sensor networks (MWSNs) have become an area of intense research activity due to technical advances in sensors, wireless communications and networking, and signal processing. Many applications, including environment monitoring, battlefield surveillance, and urban search and rescue especially in hazardous situations, are envisaged. However, MWSNs may be vulnerable to malicious interference because of the large-scale characteristics. When a contaminated node communications with its neighbors, multiple copies of the malware are transmitted to its neighbors, which may destroy, block regular communications, or even damage the integrity of regular data packets. Modeling spatial distribution of malware propagation over time is the first step to predict the trend of malware propagation in MWSNs. We propose a novel wireless malware propagation model with the discrete time delay based on reaction–diffusion equations in mobile wireless sensor networks, and study its dynamic behaviors. By analyzing the stability and Hopf bifurcation of the equilibrium of our model, we search for the sufficient conditions, which leads to the malware propagation disappears or continues. Furthermore, we demonstrate that oscillations in this model occur through the destabilization of the stationary solution at a Hopf bifurcation point. And formulas for determining the stability of the bifurcating periodic oscillations are derived by applying the normal form method and center manifold theorem. Finally, we conduct extensive simulations on large-scale MWSNs to evaluate the proposed model. Numerical evidence shows that the spatial–temporal dynamic characteristics of malware propagation in MWSNs are closely related to the packet transmission rate, the communication rang and the mobile behavior of nodes.

1. Introduction

Over the past decade we have witnessed the evolution of wireless sensor networks (WSNs), with advancements in hardware design, communication protocols, resource efficiency, home security, battlefield surveillance and other aspects [1–4]. MWSNs, as a particular form of WSNs, have played a significant role in the execution of the application [5]. For instance, at an intelligent farm, nodes may be attached to animals to collect information, such as body temperature, blood pressure, and movement behavior [6]. The objective is to monitor the health conditions of animals in a real-time manner. MWSNs are also applied to collect information from patients in hospitals or communities in time [7]. In fact, it has been shown [8,9] that the advantages of mobile wireless sensor networks over static wireless sensor networks include better energy efficiency, improved coverage, enhanced target tracking, and superior channel capacity. However, MWSNs are becoming attacked targets owing to the characteristics of its large-scale application [10]. Injecting malware into some nodes, especially mobile

* Corresponding author.
E-mail address: hongyongz@126.com (H. Zhao).

http://dx.doi.org/10.1016/j.camwa.2015.02.004
0898-1221/

nodes, has become a serious threat [11–13]. Wireless malware is a piece of malicious software which includes computer viruses, ransomware, worms, trojan horses, rootkits and other malicious programs, used to disrupt computer operation, block regular communications between nodes, or gain access to private computer systems. In fact, malware has destroyed the stability of the networks and also declined the network performance as it being injected into some nodes. The unstable phenomena have been observed in many dynamic systems, with rhythms originating from isolated components or emerging as a property of a system as a whole [14–16].

Accurately analyse the dynamic behavior of malware propagation is significant for the real-world applications, such as defend against the wireless malware, safeguard network security, ensure system stability and so on. The dynamics research about malware propagation has now become a compelling topic. In [17], based evaluation of the spread of an epidemic on graphs with given degree distributions, a percolation theory was developed to study the final outcome of an infection spread. The authors in [18] proposed a spatial–temporal model for characterizing malware propagation in networks based on probabilistic graphs and spatial–temporal random processes. The basic idea was to abstract malware propagation into a probabilistic graph, and described the statistical dependence of malware propagation in arbitrary topologies using a spatial–temporal random process. Based on the ordinary differential equation and the SIR model [19–22], Wang in [23, 24] derived the threshold for a piece of malware to propagate in WSNs, where all the nodes were supposed to be stationary. Recently, [25] considered a modeling framework which mathematically characterizes the process of malware propagation in MWSNs based on the theory of reaction–diffusion equation. In [25] the nodes in MWSNs were divided into three types, namely, susceptible nodes, infected nodes and recovered nodes. The model was described as the following form

$$\begin{cases} \dfrac{\partial S(x,y,t)}{\partial t} = \mu\nabla^2 S + A - \eta S - \dfrac{\pi r^2[1-(1-p)^{\rho}]}{\Phi_{x,y}} \dfrac{I}{1+\alpha I^2} IS - \varepsilon_1 S, \\ \dfrac{\partial I(x,y,t)}{\partial t} = \mu\nabla^2 I + \dfrac{\pi r^2[1-(1-p)^{\rho}]}{\Phi_{x,y}} \dfrac{I}{1+\alpha I^2} SI - \eta I - \varepsilon_2 I, \\ \dfrac{\partial R(x,y,t)}{\partial t} = \mu\nabla^2 R + \varepsilon_1 S + \varepsilon_2 I - \eta R, \\ s.t. \\ \dfrac{\partial S}{\partial \phi} = \dfrac{\partial I}{\partial \phi} = \dfrac{\partial R}{\partial \phi} = 0, \quad (x, y \in \partial\Omega), \\ I^0 > 0, \qquad S^0 > 0, \quad R^0 = 0, \end{cases} \tag{1.1}$$

where Ω is the network region, $\partial\Omega$ is the boundary of Ω, ϕ is the outside normal vector of $\partial\Omega$, $S(x,y,t)$, $I(x,y,t)$ and $R(x,y,t)$ are the number of susceptible nodes, infected nodes and recovered nodes in block (x,y) at instant t, respectively, and A, ε_1, ε_2, η, ρ, p, α, μ, r, $\Phi_{x,y}$ are positive constants. The constant A is the rate at which new nodes are added into a MWSN, ε_1 is the probability with which a susceptible node becomes a recovered node, ε_2 is the probability with which an infected node becomes a recovered node, η is the dead rate of nodes, ρ is the packet transmission rate of each node, p is the packet transmission probability between neighbors, α is the adjusting factor related to the network environment, μ is the diffusion coefficient, r is the communication radius, $\Phi_{x,y}$ is the area of block (x,y). ∇^2 denotes the Laplacian operator, namely, $\nabla^2 = \partial^2/\partial x^2 + \partial^2/\partial y^2$. S^0, I^0 and R^0 are the initial density of susceptible nodes, infected nodes and recovered nodes, respectively.

In fact, in MWSNs, when a susceptible node is infected by a node, there is a time $\tau > 0$ during which the infectious agents develop in the node and it is only after that time that the infected node becomes itself infectious. In this work, it is assumed that the number of the vector nodes is very large and at any time t the number of the susceptible nodes is simply proportional to the number of the infected nodes at time $t-\tau$. Thus, if we denote by $S(x,y,t)$ the susceptible nodes and by $I(x,y,t)$ the infected nodes, the force of infection at time t is assumed to be given by $\beta SI(t-\tau)$, where β is the rate at which, when having a connection to one infected node, one susceptible node can become infected. Here, we assume that $\Omega = [0,L]\times[0,L]$, l, α and κ represent the 2-D region of a MWSN, the communication radius of each node, the packet transmission rate of wireless malware and the number of wireless malware in each node, respectively. Then we have $\beta = \frac{\pi l^2[1-(1-\alpha)^{\kappa}]}{L^2}$. At the same time, in [26–28], we find that the susceptible individuals are usually assumed to have logistic growth with carrying capacity $k > 0$ as well as an intrinsic growth rate $r > 0$.

Inspired by the above mentioned work, this paper deals with a novel SIR model of wireless malware propagation in MWSNs, which is of the following form

$$\begin{cases} \dfrac{\partial S}{\partial t} = d\nabla^2 S + rS\left(1 - \dfrac{S}{k}\right) - \beta SI(t-\tau) - \varepsilon_1 S - \eta S, \\ \dfrac{\partial I}{\partial t} = d\nabla^2 I + \beta SI(t-\tau) - \varepsilon_2 I - \eta I, \\ \dfrac{\partial R}{\partial t} = d\nabla^2 R + \varepsilon_1 S + \varepsilon_2 I - \eta R, \\ 0 < x, y < L, \quad t > 0, \\ \dfrac{\partial S}{\partial \phi} = \dfrac{\partial I}{\partial \phi} = \dfrac{\partial R}{\partial \phi} = 0, \quad x, y = 0, L, \ t \geq 0, \end{cases} \tag{1.2}$$

with initial conditions

$$\begin{cases} S(x,y,t) = \psi_1(x,y,t) \geq 0, \\ I(x,y,t) = \psi_2(x,y,t) \geq 0, \\ R(x,y,t) = \psi_3(x,y,t) \geq 0, \\ (x,y,t) \in [0,L] \times [0,L] \times [-\tau, 0], \end{cases} \tag{1.3}$$

where $d > 0, k > 0$ and $r > 0$ denote the diffusion ability of mobile nodes, the most carrying capacity of the mobile wireless sensor networks and the intrinsic growth rate of the susceptible nodes, respectively; the Neumann boundary condition $\frac{\partial S}{\partial \phi} = \frac{\partial I}{\partial \phi} = \frac{\partial R}{\partial \phi} = 0$ represents no communication between nodes across the boundaries; $\psi_1(x,y,t)$, $\psi_2(x,y,t)$ and $\psi_3(x,y,t)$ are the initial density of susceptible nodes, infected nodes and recovered nodes, respectively. And the other parameters are the same means as system (1.1). In the initial condition (1.3), we assume that

$$\psi_j(x,y,t) \in \mathcal{C} = C(X, [-\tau, 0]), \quad (j = 1, 2, 3)$$

and X is defined by

$$X = \left\{ (S, I, R) \in [C^1(\bar{\Omega})]^3 : \frac{\partial S}{\partial \phi} = \frac{\partial I}{\partial \phi} = \frac{\partial R}{\partial \phi} = 0 \text{ on } \partial\Omega \right\}.$$

Because the first two equations in (1.2) are independent of $R(x,y,t)$, we can consider the following reduced model:

$$\begin{cases} \dfrac{\partial S}{\partial t} = d\nabla^2 S + rS\left(1 - \dfrac{S}{k}\right) - \beta SI(t-\tau) - \varepsilon_1 S - \eta S, \\ \dfrac{\partial I}{\partial t} = d\nabla^2 I + \beta SI(t-\tau) - \varepsilon_2 I - \eta I, \\ 0 < x, y < L, \quad t > 0, \\ \dfrac{\partial S}{\partial \phi} = \dfrac{\partial I}{\partial \phi} = 0, \quad x, y = 0, L, \ t \geq 0, \end{cases} \tag{1.4}$$

with initial conditions

$$\begin{cases} S(x,y,t) = \psi_1(x,y,t) \geq 0, \\ I(x,y,t) = \psi_2(x,y,t) \geq 0, \\ (x,y,t) \in [0,L] \times [0,L] \times [-\tau, 0]. \end{cases} \tag{1.5}$$

In this paper, we will study the stability of system (1.4) and demonstrate that oscillations in this model occur through the destabilization of the stationary solution at a Hopf bifurcation point. Here, in system (1.4) we choose delay τ as the bifurcation parameter. For simplicity, in (1.4) and (1.5), we choose $L = \pi$. Our main contributions are summarized as follows.

(1) Through the analysis of the mechanism of malware propagation in MWSNs, we generally quantify the process of malware propagation in MWSNs based on the SIR model in the epidemic theory, and then we develop a delayed malware propagation model with logistic process in MWSNs based on the reaction–diffusion equation. At the same time, we conduct extensive simulations on large-scale MWSNs to evaluate the proposed model. Numerical evidence shows that the spatial–temporal dynamic characteristics of malware propagation in MWSNs are closely related to the packet transmission rate, the communication rang and the mobile behavior of nodes.

(2) Through the stability and Hopf bifurcation analysis of the equilibrium points for the proposed model, we obtain the sufficient conditions whether a piece of malware propagates or dies out in MWSNs. When the system occurs periodic oscillation, based on the normal form method and center manifold theorem we analysis the property of periodic oscillation. Thus, we can prevent or decrease malware propagation by adjusting the values of some network parameters.

The structure of this paper is arranged as follows. In Section 2, we consider the existence, uniqueness of nonnegative solutions of system (1.4). In Section 3, we study the local stability of and the existence of Hopf bifurcation. In Section 4, we give formula determining the direction of Hopf bifurcation and the stability of spatially homogeneous bifurcating periodic solutions. Finally, to support our theoretical predictions, some numerical simulations are given which support the analysis of Sections 3 and 4.

2. The existence, uniqueness of nonnegative solutions

In this section, we will discuss the existence, uniqueness of nonnegative solutions. To do so, we need the following concepts and results.

Definition 1. A pair of smooth functions $\bar{U} = (\bar{S}, \bar{I})^T$ and $\underline{U} = (\underline{S}, \underline{I})^T$ are called upper–lower solutions of (1.4), if $\bar{S} > \underline{S}, \bar{I} > \underline{I}$ in $[0, \pi] \times [0, \pi] \times [-\tau, \infty)$ and the following differential inequalities hold

$$\begin{cases} \dfrac{\partial \bar{S}}{\partial t} - d\nabla^2 \bar{S} \geq r\bar{S}(1 - \bar{S}/k) - \beta \bar{S}\underline{I}(t-\tau) - \eta \bar{S} - \varepsilon_1 \bar{S}, \\ \dfrac{\partial \bar{I}}{\partial t} - d\nabla^2 \bar{I} \geq \beta \bar{S}\bar{I}(t-\tau) - \eta \bar{I} - \varepsilon_2 \bar{I}, \\ \dfrac{\partial \underline{S}}{\partial t} - d\nabla^2 \underline{S} \leq r\underline{S}(1 - \underline{S}/k) - \beta \underline{S}\bar{I}(t-\tau) - \eta \underline{S} - \varepsilon_1 \underline{S}, \\ \dfrac{\partial \underline{I}}{\partial t} - d\nabla^2 \underline{I} \leq \beta \underline{S}\,\underline{I}(t-\tau) - \eta \underline{I} - \varepsilon_2 \underline{I}, \\ \underline{S}(x, y, t) \leq \psi_1(x, y, t) \leq \bar{S}(x, y, t), \qquad \underline{I}(x, y, t) \leq \psi_2(x, y, t) \leq \bar{I}(x, y, t). \end{cases} \tag{2.1}$$

Furthermore, we make following assumptions

(H_1) $r > \eta + \varepsilon_1$,
(H_2) $k\beta(r - \eta - \varepsilon_1) - 3r(\eta + \varepsilon_2) > 0$.

Lemma 1 (*[29]*). *Let $\bar{U}$ and $\underline{U}$ be a pair of coupled upper and lower solutions for system (1.4) and suppose that the initial functions $\psi_i (i = 1, 2)$ are Hölder continuous in $[0, \pi] \times [0, \pi] \times [-\tau, 0]$. Then system (1.4) has exactly one regular solution $\widehat{U}(x, y, t) = (S(x, y, t), I(x, y, t))^T$ satisfying $\underline{U} \leq \widehat{U} \leq \bar{U}$ in $[0, \pi] \times [0, \pi] \times [-\tau, \infty)$ as (H_1) and (H_2) hold.*

Proof. Let $\underline{U} = (0, 0)^T$ and $\bar{U} = (\bar{S}, \bar{I})^T$, where $\bar{S}, \bar{I}$ satisfy

$$\begin{cases} \bar{S} > \max\left\{ \|\psi_1\|, \dfrac{k(r - \eta - \varepsilon_1)}{r}, \dfrac{\eta + \varepsilon_2}{\beta} \right\}, \\ \bar{I} > \|\psi_2\|, \end{cases} \tag{2.2}$$

where $\|\psi_i\| = \sup_{(x,y,t) \in \bar{\Omega} \times [-\tau, 0]} |\psi_i(x, y, t)|, (i = 1, 2)$. Then $\underline{U} = (0, 0)^T$ and $\bar{U} = (\bar{S}, \bar{I})^T$ are clearly a pair of lower–upper solution of (1.4), therefore, $0 \leq S(x, y, t) \leq \bar{S}$, $0 \leq I(x, y, t) \leq \bar{I}$ for $(x, y, t) \in [0, \pi] \times [0, \pi] \times [-\tau, \infty]$. Furthermore, by the maximal principle, we have $S(x, y, t) > 0$ and $I(x, y, t) > 0$ for all $t > 0$, $x, y \in [0, \pi]$, if $\psi_i(x, y, 0) > 0$ $(i = 1, 2)$. This completes the proof.

3. Local stability and Hopf bifurcation

In this section, we will discuss the local stability and Hopf bifurcation of system (1.4) with the time delay τ as the bifurcation parameter by analyzing the corresponding characteristic equations. First, we make the following assumptions

(H_3) $r(r + \varepsilon_2 - \varepsilon_1) + k\beta(\eta + \varepsilon_1 - r) > 0$,
(H_4) $k\beta(\eta + \varepsilon_1 - r) + r(\eta + \varepsilon_2) > 0$,
(H_5) $r(\eta + \varepsilon_2) + k\beta(\varepsilon_1 - \varepsilon_2) > 0$,
(H_6) $r^2(\eta + \varepsilon_2) + k\beta(\varepsilon_1 - \varepsilon_2)(2r + k\beta) > 0$,
(H_7) $d^2 + k^2\beta^2(\eta + \varepsilon_1 - r)(\eta + \varepsilon_2) > 0$.

It can be seen that homogeneous Neumann boundary conditions imposed on (1.4) lead to $E^0 = (0, 0)^T$ being the trivial equilibrium point for any feasible parameters, $E^1 = (\hat{S}, 0)^T$ always being the malware-free equilibrium point under the condition (H_1), where

$$\hat{S} = \frac{k(r - \eta - \varepsilon_1)}{r};$$

and (1.4) always having a unique positive equilibrium point $E^* = (S^*, I^*)^T$ provided that the condition (H_2) holds, where

$$S^* = \frac{\eta + \varepsilon_2}{\beta}, \qquad I^* = \frac{kr\beta - k\beta\eta - k\beta\varepsilon_1 - r\eta - r\varepsilon_2}{k\beta^2}.$$

Let $\tilde{S} = S - S^\star$, $\tilde{I} = I - I^\star$, where $(S^\star, I^\star)^T$ is an arbitrary equilibrium point, and drop bars for the simplicity of notations. Then system (1.4) can be transformed into the following form

$$\begin{cases} \dfrac{\partial S}{\partial t} = d\nabla^2 S + \left(r - \eta - \varepsilon_1 - \dfrac{2rS^\star}{k} - \beta I^\star \right) S - \beta S^\star I(t-\tau) - \dfrac{r}{k} S^2 - \beta S I(t-\tau), \\ \dfrac{\partial I}{\partial t} = d\nabla^2 I + \beta I^\star S - (\eta + \varepsilon_2) I + \beta S^\star I(t-\tau) + \beta S I(t-\tau), \\ 0 < x < \pi, \quad 0 < y < \pi, \quad t > 0, \\ \dfrac{\partial S}{\partial x}(x, y, t) = \dfrac{\partial I}{\partial x}(x, y, t) = 0, \qquad \dfrac{\partial S}{\partial y}(x, y, t) = \dfrac{\partial I}{\partial y}(x, y, t) = 0, \quad x = 0, \pi, \ y = 0, \pi, \ t \geq 0. \end{cases} \tag{3.1}$$

Thus, the arbitrary equilibrium point $E^\star = (S^\star, I^\star)^T$ of system (1.4) is transformed into the zero equilibrium point $(0, 0)^T$ of system (3.1).

In the following, we will analysis stability and bifurcation of the zero equilibrium point of system (3.1).

Denote

$$U(t) = (u_1(t), u_2(t))^T = (S(\cdot, \cdot, t), I(\cdot, \cdot, t))^T,$$

then (3.1) can be rewritten as an abstract differential equation in the phase space $\mathcal{C} = C(X, [-\tau, 0])$ of the form

$$\dot{U} = D\Delta U(t) + L(U_t) + f(U_t), \tag{3.2}$$

where

$D = diag\{d, d\}$,
$\Delta = diag\{\partial^2/\partial x^2 + \partial^2/\partial y^2, \partial^2/\partial x^2 + \partial^2/\partial y^2\}$,
$U_t(\theta) = U(t + \theta)$, $-\tau \le \theta \le 0$,
$L : \mathcal{C} \to X$

and

$f : \mathcal{C} \to X$ are given, respectively, by

$$L(\varphi) = \begin{pmatrix} \left(r - \eta - \varepsilon_1 - \dfrac{2S^\star r}{k} - \beta I^\star\right)\varphi_1(0) - \beta S^\star \varphi_2(-\tau) \\ \beta I^\star \varphi_1(0) - (\eta + \varepsilon_2)\varphi_2(0) + \beta S^\star \varphi_2(-\tau) \end{pmatrix} \tag{3.3}$$

and

$$f(\varphi) = \begin{pmatrix} -\dfrac{r}{k}\varphi_1^2(0) - \beta\varphi_1(0)\varphi_2(-\tau) \\ \beta\varphi_1(0)\varphi_2(-\tau) \end{pmatrix}. \tag{3.4}$$

For $\varphi(\theta) = U_t(\theta)$, $\varphi = (\varphi_1, \varphi_2)^T \in \mathcal{C}$, the linearized system of (3.2) at the zero equilibrium point is

$$\dot{U} = D\Delta U(t) + L(U_t) \tag{3.5}$$

and its characteristic equation is

$$\lambda w - D\Delta w - L(e^{\lambda \cdot} w) = 0, \tag{3.6}$$

where $w \in dom(\Delta)$, and $w \ne 0$, $dom(\Delta) \subset X$.

From the properties of the Laplacian operator defined on the bounded domain, the operator Δ on X has the eigenvalues $-(m^2 + n^2)$, $(m, n \in N_0 \triangleq \{0, 1, 2 \cdots\})$ with the relative eigenfunctions on X are

$$\beta_{mn}^1 = (\gamma_{mn}, 0)^T, \qquad \beta_{mn}^2 = (0, \gamma_{mn})^T,$$

where

$$\gamma_{mn} = \cos(mx)\cos(ny).$$

Clearly, $(\beta_{mn}^1, \beta_{mn}^2)_0^\infty$ construct a basis of the phase space X. Therefore, any element w in X can be expanded as Fourier series in the following form

$$w = \sum_{m,n=0}^{\infty} W_{mn}^T \begin{pmatrix} \beta_{mn}^1 \\ \beta_{mn}^2 \end{pmatrix}, \qquad W_{mn} = \begin{pmatrix} \langle w, \beta_{mn}^1 \rangle \\ \langle w, \beta_{mn}^2 \rangle \end{pmatrix}. \tag{3.7}$$

By calculation

$$L(\varphi^T(\beta_{mn}^1, \beta_{mn}^2)^T) = L(\varphi)^T(\beta_{mn}^1, \beta_{mn}^2), \quad m, n \in N_0. \tag{3.8}$$

According to (3.7) and (3.8), (3.6) is equivalent to

$$\sum_{m,n=0}^{\infty} W_{mn}^T \left[\lambda I_2 + D(m^2 + n^2) - \begin{pmatrix} r - \eta - \varepsilon_1 - \dfrac{2S^\star r}{k} - \beta I^\star & \beta I^\star \\ -\beta S^\star e^{-\lambda\tau} & -(\eta + \varepsilon_2) + \beta S^\star e^{-\lambda\tau} \end{pmatrix}\right] \begin{pmatrix} \beta_{mn}^1 \\ \beta_{mn}^2 \end{pmatrix} = 0. \tag{3.9}$$

Hence, we conclude that (3.9) is equivalent to the following form

$$\lambda^2 + [2d(m^2 + n^2) + A_1]\lambda + [d^2(m^2 + n^2)^2 + A_1 d(m^2 + n^2) + A_2] + [A_3\lambda + A_3 d(m^2 + n^2) + A_4]e^{-\lambda\tau} = 0, \tag{3.10}$$

where

$$A_1 = 2\eta + \varepsilon_1 + \varepsilon_2 + \frac{2S^\star r}{k} + \beta I^\star - r,$$
$$A_2 = \eta^2 + \varepsilon_1\eta + \varepsilon_2\eta + \varepsilon_1\varepsilon_2 + \frac{2S^\star r\eta}{k} + \frac{2S^\star r\varepsilon_2}{k} + \beta I^\star\eta + \beta I^\star\varepsilon_2 - r\eta - r\varepsilon_2,$$
$$A_3 = -\beta S^\star,$$
$$A_4 = \beta S^\star r - \beta S^\star\eta - \beta S^\star\varepsilon_1 - \frac{2S^{\star^2} r\beta}{k}.$$

Theorem 1 (*Harmless Delays on the Malware Propagation in MWSNs*). *If* (H_1) *holds. Assume furthermore that* (H_3)–(H_4) *satisfy. Then the malware-free equilibrium point* E^1 *of system* (1.4) *is locally asymptotically stable for* $\forall\tau \geq 0$.

Proof. The characteristic equation of system (1.4) about the malware-free equilibrium point $E^1 = (\hat{S}, 0)^T$ takes the form

$$\lambda^2 + [2d(m^2+n^2) + B_1]\lambda + [d^2(m^2+n^2)^2 + B_1 d(m^2+n^2) + B_2] + [B_3\lambda + B_3 d(m^2+n^2) + B_4]e^{-\lambda\tau} = 0, \quad (3.11)$$

where

$$B_1 = r - \varepsilon_1 + \varepsilon_2,$$
$$B_2 = r\eta + r\varepsilon_2 - \varepsilon_1\eta - \varepsilon_2\eta - \varepsilon_1\varepsilon_2 - \eta^2,$$
$$B_3 = -\frac{k\beta(r - \eta - \varepsilon_1)}{r},$$
$$B_4 = -\frac{k\beta}{r}(r^2 + \eta^2 + \varepsilon_1^2 + 2\eta\varepsilon_1 - 2r\eta - 2r\varepsilon_1).$$

Obviously, for $\forall m, n \in N_0$, $\lambda = 0$ is not a root of (3.11). And as $\tau = 0$, Eq. (3.11) is equivalent to the following quadratic equation

$$\lambda^2 + [2d(m^2+n^2) + B_1 + B_3]\lambda + [d^2(m^2+n^2)^2 + d(B_1+B_3)(m^2+n^2) + B_2 + B_4] = 0. \quad (3.12)$$

By (H_3), we obtain that

$$B_1 + B_3 = (r - \varepsilon_1) + \frac{k\beta}{r}(\eta + \varepsilon_1 - r) + \varepsilon_2 > 0.$$

By (H_1) and (H_4), we have

$$B_2 + B_4 = (r - \eta - \varepsilon_1)\left[\eta + \varepsilon_2 + \frac{k\beta(\eta + \varepsilon_1 - r)}{r}\right] > 0.$$

Then, for $\forall m, n \in N_0$, it is easy to show that

$$2d(m^2+n^2) + B_1 + B_3 \geq B_1 + B_3 > 0$$

and

$$d^2(m^2+n^2)^2 + d(B_1+B_3)(m^2+n^2) + B_2 + B_4 \geq B_2 + B_4 > 0.$$

According to the Routh–Hurwitz criteria, all the roots of Eq. (3.12) have negative real parts. Therefore, the malware-free equilibrium point E^1 is locally asymptotically stable. Next we discuss the effect of the delay τ on the stability of the trivial solution of (3.11). Assume that $i\omega$ is a root of Eq. (3.11). Then ω should satisfy the following equation for $m, n \in N_0$

$$-\omega^2 + i\omega[2d(m^2+n^2) + B_1] + [d^2(m^2+n^2)^2 + B_1 d(m^2+n^2) + B_2] + [iB_3\omega + B_3 d(m^2+n^2) + B_4]e^{-i\omega\tau} = 0, \quad (3.13)$$

which implies that

$$\begin{cases} B_3\omega\sin\omega\tau + [B_3 d(m^2+n^2) + B_4]\cos\omega\tau = \omega^2 - [d^2(m^2+n^2) + B_1 d(m^2+n^2) + B_2], \\ B_3\omega\cos\omega\tau - [B_3 d(m^2+n^2) + B_4]\sin\omega\tau = \omega[2d(m^2+n^2) + B_1]. \end{cases} \quad (3.14)$$

Taking square on both sides of the equations of (3.14) and summing then up, we obtain

$$\omega^4 + [2d^2(m^2+n^2)^2 + 2B_1 d(m^2+n^2) + B_1^2 - B_3^2 - 2B_2]\omega^2 + [d^2(m^2+n^2)^2 + (B_1+B_3)d(m^2+n^2) + B_2 + B_4][d^2(m^2+n^2)^2 + (B_1 - B_3)d(m^2+n^2) + B_2 - B_4] = 0. \quad (3.15)$$

Set $z = \omega^2$, Eq. (3.15) is transformed into the following equation

$$z^2 + [2d^2(m^2+n^2)^2 + 2B_1d(m^2+n^2) + B_1^2 - B_3^2 - 2B_2]z + [d^2(m^2+n^2)^2 + d(B_1+B_3)(m^2+n^2) + B_2 + B_4][d^2(m^2+n^2)^2 + d(B_1-B_3)(m^2+n^2) + B_2 - B_4] = 0. \tag{3.16}$$

When $m^2+n^2 = 0$, Eq. (3.16) becomes

$$z^2 + (B_1^2 - B_3^2 - 2B_2)z + B_2^2 - B_4^2 = 0. \tag{3.17}$$

Clearly,

$$B_2^2 - B_4^2 = (B_2+B_4)(B_2-B_4) > 0.$$

If Eq. (3.17) has a positive solution, then the following conditions must hold

(i) $B_1^2 - B_3^2 - 2B_2 < 0$,
(ii) $(B_1^2 - B_3^2 - 2B_2)^2 - 4(B_2^2 - B_4^2) > 0$.

That is,

$$r(r-2\varepsilon_2-2\eta) + \varepsilon_1^2 + \varepsilon_2^2 + 2\eta(\eta+\varepsilon_1+\varepsilon_2) - \frac{k^2\beta^2(r-\eta-\varepsilon_1)^2}{r^2} + 2(r-\eta-\varepsilon_1)\sqrt{(\eta+\varepsilon_2)^2 - \frac{k^2\beta^2(r-\eta-\varepsilon_1)^2}{r^2}} < 0.$$

Let

$$P = r(r-2\varepsilon_2-2\eta) + \varepsilon_1^2 + \varepsilon_2^2 + 2\eta(\eta+\varepsilon_1+\varepsilon_2) - \frac{k^2\beta^2(r-\eta-\varepsilon_1)^2}{r^2} + 2(r-\eta-\varepsilon_1)\sqrt{(\eta+\varepsilon_2)^2 - \frac{k^2\beta^2(r-\eta-\varepsilon_1)^2}{r^2}}.$$

Under the condition (H_4), we have

$$\begin{aligned} P &> r(r-\eta-\varepsilon_1) - r(\eta+\varepsilon_1) + \varepsilon_1^2 + \varepsilon_2^2 - (\eta+\varepsilon_2)^2 + 2(r-\eta-\varepsilon_1)\sqrt{(\eta+\varepsilon_2)^2 - \frac{k^2\beta^2(r-\eta-\varepsilon_1)^2}{r^2}} \\ &= r(r-\eta-\varepsilon_1) - r(\eta+\varepsilon_1) + (\eta+\varepsilon_1)^2 + 2(r-\eta-\varepsilon_1)\sqrt{(\eta+\varepsilon_2)^2 - \frac{k^2\beta^2(r-\eta-\varepsilon_1)^2}{r^2}} \\ &= (r-\eta-\varepsilon_1)^2 + 2(r-\eta-\varepsilon_1)\sqrt{(\eta+\varepsilon_2)^2 - \frac{k^2\beta^2(r-\eta-\varepsilon_1)^2}{r^2}} > 0, \end{aligned}$$

which is a contradiction to $P < 0$. Then, Eq. (3.17) has no positive solutions. Moreover, there are no positive solutions for Eq. (3.15).

When $m^2+n^2 \geq 1$, similarly, we can obtain that Eq. (3.15) has no positive solutions. Therefore, the malware-free equilibrium point E^1 is locally asymptotically stable for $\forall\tau \geq 0$. This completes proof.

For the positive equilibrium point $E^* = (S^*, I^*)^T$, (3.10) reduces to

$$\lambda^2 + [2d(m^2+n^2) + C_1]\lambda + [d^2(m^2+n^2)^2 + C_1d(m^2+n^2) + C_2] + [C_3\lambda + C_3d(m^2+n^2) + C_4]e^{-\lambda\tau} = 0, \tag{3.18}$$

where

$$\begin{aligned} C_1 &= \frac{r(\eta+\varepsilon_2)}{k\beta} + \eta + \varepsilon_1, \\ C_2 &= (\eta+\varepsilon_2)\left(\eta + \varepsilon_1 + \frac{r\eta + r\varepsilon_2 - k\beta\eta - k\beta\varepsilon_1}{k\beta}\right), \\ C_3 &= -\eta - \varepsilon_2, \\ C_4 &= \frac{1}{k\beta}(\eta+\varepsilon_2)[k\beta(r-\eta-\varepsilon_1) - 2r(\eta+\varepsilon_2)]. \end{aligned}$$

Lemma 2 (*Without Delays on the Malware Propagation in MWSNs*). *If the conditions* (H_2) *and* (H_5) *hold, then system* (1.4) *is locally asymptotically stable at the positive equilibrium point* E^* *as* $\tau = 0$.

Proof. Obviously, for $\forall m, n \in N_0$, $\lambda = 0$ is not a root of (3.18). As $\tau = 0$, Eq. (3.18) is equivalent to the following quadratic equation

$$\lambda^2 + [2d(m^2+n^2) + C_1 + C_3]\lambda + [d^2(m^2+n^2)^2 + d(C_1+C_3)(m^2+n^2) + C_2 + C_4] = 0. \tag{3.19}$$

Clearly, from (H_5), we have

$$C_1 + C_3 = \frac{r(\eta+\varepsilon_2) + k\beta(\varepsilon_1-\varepsilon_2)}{k\beta} > 0,$$

and by (H_2), we obtain

$$C_2 + C_4 = \frac{r(\eta+\varepsilon_2)^2}{k\beta} + \frac{1}{k\beta}(\eta+\varepsilon_2)[k\beta(r-\eta-\varepsilon_2) - 2r(\eta+\varepsilon_2)] > 0.$$

Therefore, for $\forall m, n \in N_0$, it is easy to obtain that

$$2d(m^2+n^2) + C_1 + C_3 \geq C_1 + C_3 > 0$$

and

$$d^2(m^2+n^2)^2 + d(C_1+C_3)(m^2+n^2) + C_2 + C_4 \geq C_2 + C_4 > 0.$$

According to the Routh–Hurwitz criteria, all the roots of Eq. (3.19) have negative real parts. Therefore, when $\tau = 0$, the positive equilibrium point E^* is locally asymptotically stable.

Theorem 2 (*Harmful Delays on the Malware Propagation in MWSNs*)**.** *If* (H_2) *holds. Assume furthermore that* (H_5)–(H_7) *satisfy. Then for system* (1.4)*, the following statements are true.*

(i) *When* $\tau \in [0, \tau_0^0)$*, the positive equilibrium point* E^* *of system* (1.4) *is locally asymptotically stable.*

(ii) *The Hopf bifurcation occurs when* $\tau = \tau_0^j$*. That is, system* (1.4) *has a branch of periodic solutions bifurcating from the positive equilibrium point* E^* *near* $\tau = \tau_0^j$*, where*

$$\tau_0^j = \frac{1}{\omega_0}\left(\arccos\frac{(C_4 - C_1C_3)\omega_0^2 - C_2C_4}{C_3^2\omega_0^2 + C_4^2} + 2j\pi\right) \quad (j = 0, 1, 2\cdots),$$

$$\omega_0 = \left[\frac{C_3^2 + 2C_2 - C_1^2 + \sqrt{(C_3^2 + 2C_2 - C_1^2)^2 - 4(C_2^2 - C_4^2)}}{2}\right]^{\frac{1}{2}}.$$

Proof. Clearly, $\lambda = 0$ is not a solution of (3.18). In fact, if $\lambda = 0$, then (3.18) becomes

$$d(C_1+C_3)(m^2+n^2) + C_2 + C_4 = 0,$$

which is a contradiction to

$$d(C_1+C_3)(m^2+n^2) + C_2 + C_4 \geq C_2 + C_4 > 0.$$

Next we discuss the effect of the delay τ on the stability of the trivial solution of (3.18). Assume that $i\omega(\omega > 0)$ is a root of Eq. (3.18). Then ω should satisfy the following equation for some $m, n \in N_0$

$$\begin{aligned} &-\omega^2 + i\omega[2d(m^2+n^2) + C_1] + [d^2(m^2+n^2)^2 + C_1d(m^2+n^2) + C_2] \\ &\quad + [iC_3\omega + C_3d(m^2+n^2) + C_4]e^{-i\omega\tau} = 0, \end{aligned} \tag{3.20}$$

which leads to

$$\begin{cases} C_3\omega\sin\omega\tau + [C_3d(m^2+n^2) + C_4]\cos\omega\tau = \omega^2 - [d^2(m^2+n^2) + C_1d(m^2+n^2) + C_2], \\ C_3\omega\cos\omega\tau - [C_3d(m^2+n^2) + C_4]\sin\omega\tau = \omega[2d(m^2+n^2) + C_1]. \end{cases} \tag{3.21}$$

Taking square on both sides of the equations of (3.21) and summing then up, we obtain

$$\begin{aligned} &\omega^4 + [2d^2(m^2+n^2)^2 + 2C_1d(m^2+n^2) + C_1^2 - C_3^2 - 2C_2]\omega^2 + [d^2(m^2+n^2)^2 \\ &\quad + d(C_1+C_3)(m^2+n^2) + C_2 + C_4][d^2(m^2+n^2)^2 + d(C_1-C_3)(m^2+n^2) + C_2 - C_4] = 0. \end{aligned} \tag{3.22}$$

Let $z = \omega^2$, then (3.22) can be written as a second-degree polynomial, defined by

$$\begin{aligned} &z^2 + [2d^2(m^2+n^2)^2 + 2C_1d(m^2+n^2) + C_1^2 - C_3^2 - 2C_2]z + [d^2(m^2+n^2)^2 \\ &\quad + d(C_1+C_3)(m^2+n^2) + C_2 + C_4][d^2(m^2+n^2)^2 + d(C_1-C_3)(m^2+n^2) + C_2 - C_4] = 0. \end{aligned} \tag{3.23}$$

Under the condition (H_2), it is easy to show that

$$C_2 + C_4 > 0$$

and

$$C_2 - C_4 = \frac{1}{k\beta}(\eta + \varepsilon_2)[3r(\eta + \varepsilon_2) - k\beta(r - \eta - \varepsilon_1)] < 0.$$

Thus, when $m^2 + n^2 = 0$, Eq. (3.23) has a unique positive root, denoted by Z_0, and moreover Eq. (3.22) has a unique positive root $\omega_0 = \sqrt{Z_0}$. By (3.21), we have

$$\cos \omega_0 \tau = \frac{(C_4 - C_1C_3)\omega_0^2 - C_2C_4}{C_3^2\omega_0^2 + C_4^2}.$$

Thus, if we denote

$$\tau_0^j = \frac{1}{\omega_0}\left[\arccos \frac{(C_4 - C_1C_3)\omega_0^2 - C_2C_4}{C_3^2\omega_0^2 + C_4^2} + 2j\pi\right], \quad j = 0, 1, 2 \cdots,$$

then $\pm i\omega_0$ is a pair of purely imaginary roots of Eq. (3.18) at $\tau = \tau_0^j$.

For $m^2 + n^2 \geq 1$, assume that (H_6) holds, then we have the following result

$$2d^2(m^2 + n^2)^2 + 2C_1d(m^2 + n^2) + C_1^2 - C_3^2 - 2C_2 > 0.$$

According to Lemma 2, we can see

$$C_1 + C_3 > 0$$

and

$$C_2 + C_4 > 0,$$

then

$$d^2(m^2 + n^2)^2 + d(C_1 + C_3)(m^2 + n^2) + C_2 + C_4 > 0.$$

Clearly

$$C_1 - C_3 > 0,$$

and from (H_7), when $m^2 + n^2 = 1$, it is easy to obtain that

$$\begin{aligned} &d^2(m^2 + n^2)^2 + d(C_1 - C_3)(m^2 + n^2) + (C_2 - C_4) \\ &\quad \geq d^2 + 2\sqrt{2}r(\eta + \varepsilon_2)^2 + k^2\beta^2(\eta + \varepsilon_2)(\eta + \varepsilon_1 - r) > d^2 + k^2\beta^2(\eta + \varepsilon_2)(\eta + \varepsilon_1 - r) > 0. \end{aligned}$$

Then, it follows from the Routh–Hurwitz criteria that Eq. (3.23) has no positive root and hence Eq. (3.18) has no purely imaginary root. That is, for $\forall m, n \in N_0$, all the roots of (3.18) have negative real parts for $\tau \in [0, \tau_0^0)$, and all the roots of (3.18) except $\pm i\omega_0$ have negative real parts for $\tau = \tau_0^0$.

For applying the Hopf bifurcation theorem, we also need to verify the following transversality condition

$$\left.\frac{d(\mathrm{Re}\lambda(\tau))}{d\tau}\right|_{\tau=\tau_0^j, \lambda=i\omega_0} > 0. \tag{3.24}$$

In fact,

$$\begin{aligned} \left.\frac{d(\mathrm{Re}\lambda(\tau))}{d\tau}\right|_{\tau=\tau_0^j, \lambda=i\omega_0} &= \frac{1}{\omega_0(C_3^2\omega_0^2 + C_4^2)}(2C_3\omega_0^2 \sin \omega_0\tau_0^j - C_1C_3\omega_0 \cos \omega_0\tau_0^j \\ &\quad - C_3^2\omega_0 + 2C_4\omega_0 \cos \omega_0\tau_0^j + C_1C_4 \sin \omega_0\tau_0^j) \\ &= \frac{1}{(C_3^2\omega_0^2 + C_4^2)^2}[2C_3^2\omega_0^4 + (2C_4^2 + C_1^2C_3^2 - C_3^4 - 2C_2C_3^2)\omega_0^2 + C_1^2C_4^2 - C_3^2C_4^2 - 2C_2C_4^2] \\ &= \frac{1}{(C_3^2\omega_0^2 + C_4^2)^2}\left[\frac{1}{2}C_3^2(C_3^2 + 2C_2 - C_1^2)^2\right. \\ &\quad + \frac{1}{2}C_3(C_3^2 + 2C_2 - C_1^2)\sqrt{(C_3^2 + 2C_2 - C_1^2)^2 - 4(C_2^2 - C_4^2)} \\ &\quad \left. + C_4^2\sqrt{(C_3^2 + 2C_2 - C_1^2)^2 - 4(C_2^2 - C_4^2)} + 2C_3^2(C_4^2 - C_2^2)\right] > 0. \end{aligned}$$

According to the theory of Hopf bifurcation, Theorem 2 is true.

Remark 3.1. From Theorem 2 we have obtained the local stability and Hopf bifurcation of system (1.4). In future, we will discuss the global stability of system (1.4) for $\tau \in [0, \tau_0^0)$. Furthermore, for $\forall \tau \geq 0$ the sufficient conditions for the global stability of the positive equilibrium point of the proposed problem can be derived by the Lyapunov functional or the upper and lower solutions method.

4. Direction and stability of bifurcating periodic oscillations

In the previous section, we have shown that system (3.1) admits a series of periodic solutions bifurcating from the zero equilibrium point at the critical value τ_0^j ($j \in N_0$). As we all know, the periodic oscillation in the MWSNs may destroy, block regular communications, or even damage the integrity of regular data packets. Thus, understanding the properties of the periodic oscillation, such as stability, direction and monotonicity of the periodicity, is necessary. In this section, we derive explicit formulae to determine the properties of the Hopf bifurcation at critical value $\tau_0^j (j \in N_0)$ by using the normal form theory and center manifold reduction for PFDEs developed by [30–32]. Throughout this section, we also assume that the condition (H_2) holds.

For fixed $j \in N_0$, denote τ_0^j by τ^* and introduce the new parameter $\mu = \tau - \tau^*$. Normalizing the delay τ by the time-scaling $t \to t/\tau$. Then at the positive equilibrium point E^*, (3.1) can be rewritten as

$$\frac{dU(t)}{dt} = \tau^* D\Delta U(t) + L(\tau^*)(U_t) + F(U_t, \mu), \tag{4.1}$$

where $L(\mu)(\varphi) : \mathcal{C} \to X$ and $F(\cdot, \mu) : \mathcal{C} \to X$ are given by

$$L(\mu)(\varphi) = \mu \begin{pmatrix} \left(r - \eta - \varepsilon_1 - \dfrac{2S^* r}{k} - \beta I^*\right)\varphi_1(0) - \beta S^* \varphi_2(-1) \\ \beta I^* \varphi_2(0) - (\eta + \varepsilon_2)\varphi_2(0) + \beta S^* \varphi_2(-1) \end{pmatrix}, \tag{4.2}$$

$$F(\varphi, \mu) = \mu D\Delta\varphi(0) + L(\mu)\varphi + f(\varphi, \mu) \tag{4.3}$$

and

$$f(\varphi, \mu) = (\tau^* + \mu) \begin{pmatrix} -\dfrac{r}{k}\varphi_1^2(0) - \beta\varphi_1(0)\varphi_2(-1) \\ \beta\varphi_1(0)\varphi_2(-1) \end{pmatrix}, \tag{4.4}$$

for $\varphi = (\varphi_1, \varphi_2)^T \in \mathcal{C}$.

Then linearized system of (4.1) at $(0, 0)^T$ is

$$\frac{dU(t)}{dt} = \tau^* D\Delta U(t) + L(\tau^*)(U_t). \tag{4.5}$$

Based on the discussion in Section 3, we can easily know that for $\tau = \tau^*$, $m = 0$, $n = 0$, the characteristic equation of (3.18) has a pair of simple purely imaginary eigenvalues $\Lambda_0 = \{i\omega\tau^*, -i\omega\tau^*\}$.

Let $\mathcal{C} := C(\mathbb{R}^2, [-1, 0])$, consider the following FDE on $\mathcal{C}$

$$\dot{z} = L(\tau^*)(z_t). \tag{4.6}$$

Obviously, $L(\tau^*)$ is a continuous linear function mapping $C(\mathbb{R}^2, [-1, 0])$ into $\mathbb{R}^2$. By the Riesz representation theorem, there exists a 2×2 matrix function $\eta(\theta, \tau)$ $(-1 \le \theta \le 0)$, whose elements are of bounded variation such that

$$L(\tau^*)(\varphi) = \int_{-1}^{0} [d\eta(\theta, \tau^*)]\varphi(\theta), \quad \text{for } \varphi \in C. \tag{4.7}$$

In fact, we can choose

$$\eta(\theta, \tau^*) = \tau^* \begin{pmatrix} r - \eta - \varepsilon_1 - \dfrac{2S^* r}{k} - \beta I^* & 0 \\ \beta I^* & -\eta - \varepsilon_2 \end{pmatrix} \delta(\theta) - \tau^* \begin{pmatrix} 0 & -\beta S^* \\ 0 & \beta S^* \end{pmatrix} \delta(\theta + 1), \tag{4.8}$$

where δ is the Dirac delta function.

Let $A(\tau^*)$ denote the infinitesimal generator of the semigroup induced by the solutions of (4.6) and A^* be the formal adjoint of $A(\tau^*)$ under the bilinear pairing

$$\begin{aligned} (\psi, \phi) &= (\psi(0), \phi(0)) - \int_{-1}^{0} \int_{\zeta=0}^{\theta} \psi(\zeta - \theta) d\eta(\theta) \phi(\zeta) d\zeta \\ &= (\psi(0), \phi(0)) + \tau^* \int_{-1}^{0} \psi(\theta + 1) \begin{pmatrix} 0 & -\beta S^* \\ 0 & \beta S^* \end{pmatrix} \phi(\theta) d\theta, \end{aligned} \tag{4.9}$$

for $\phi \in C$, $\psi \in C^* = C(\mathbb{R}^2, [-1, 0])$. Then $A(\tau^*)$ and A^* are a pair of adjoint operators [31]. From the discussion in Section 3, we know that $A(\tau^*)$ has a pair of simple purely imaginary eigenvalues $\pm i\omega_0\tau^*$ and they are also eigenvalues of A^* since $A(\tau^*)$ and A^* are a pair of adjoint operators. Let P and P^* be the center spaces, that is, the generalized eigenspaces of $A(\tau^*)$ and A^* associated with Λ_0, respectively. Then P^* is the adjoint space of P and $dim P = dim P^* = 2$. Direct computations give the following results.

Lemma 3. *Let* $\xi = \frac{(-i\omega_0+r-\eta-\varepsilon_1-\frac{2S^*r}{k}-\beta I^*)e^{i\omega_0\tau^*}}{\beta S^*}$, $\varsigma = \frac{i\omega_0+\eta+\varepsilon_1+\frac{2S^*r}{k}+\beta I^*-r}{\beta I^*}$, *Then*

$$p_1(\theta) = e^{i\omega_0\tau^*\theta}(1,\xi)^T, \qquad p_2(\theta) = \overline{p_1(\theta)}, \quad -1 \le \theta \le 0, \tag{4.10}$$

is a basis of P *associated with* Λ_0 *and*

$$q_1(s) = (1,\varsigma)e^{-i\omega_0\tau^*s}, \qquad q_2(s) = \overline{q_1(s)}, \quad 0 \le s \le 1, \tag{4.11}$$

is a basis of Q *associated with* Λ_0.

Let $\Phi = (\Phi_1, \Phi_2)$ and $\Psi^* = (\Psi_1^*, \Psi_2^*)^T$ with

$$\begin{aligned}
\Phi_1(\theta) &= \frac{p_1(\theta)+p_2(\theta)}{2} = \begin{pmatrix} \mathrm{Re}\{e^{i\omega_0\tau^*\theta}\} \\ \mathrm{Re}\{\xi e^{i\omega_0\tau^*\theta}\} \end{pmatrix} \\
&= \begin{pmatrix} \cos\omega_0\tau^*\theta \\ \left(\frac{\omega_0}{\eta+\varepsilon_2}\cos\omega_0\tau^* + \frac{r}{k\beta}\sin\omega_0\tau^*\right)\sin\tau^*\theta + \left(\frac{\omega_0}{\eta+\varepsilon_2}\sin\omega_0\tau^* - \frac{r}{k\beta}\cos\omega_0\tau^*\right)\cos\tau^*\theta \end{pmatrix}, \\
\Phi_2(\theta) &= \frac{p_1(\theta)-p_2(\theta)}{2i} = \begin{pmatrix} \mathrm{Im}\{e^{i\omega_0\tau^*\theta}\} \\ \mathrm{Im}\{\xi e^{i\omega_0\tau^*\theta}\} \end{pmatrix} \\
&= \begin{pmatrix} \sin\omega_0\tau^*\theta \\ -\left(\frac{\omega_0}{\eta+\varepsilon_2}\cos\omega_0\tau^* + \frac{r}{k\beta}\sin\omega_0\tau^*\right)\cos\omega_0\tau^*\theta + \left(\frac{\omega_0}{\eta+\varepsilon_2}\sin\omega_0\tau^* - \frac{r}{k\beta}\cos\omega_0\tau^*\right)\sin\omega_0\tau^*\theta \end{pmatrix},
\end{aligned}$$

for $\theta \in [-1, 0]$, and

$$\begin{aligned}
\Psi_1^*(s) &= \frac{q_1(s)+q_2(s)}{2} = \begin{pmatrix} \mathrm{Re}\{e^{-i\omega_0\tau^*s}\} \\ \mathrm{Re}\{\varsigma e^{-i\omega_0\tau^*s}\} \end{pmatrix}^T = \begin{pmatrix} \cos\omega_0\tau^*s \\ \frac{r(\eta+\varepsilon_2)\cos\omega_0\tau^*s + k\beta\omega_0\sin\omega_0\tau^*s}{k\beta r - k\beta\eta - k\beta\varepsilon_1 - r\eta - r\varepsilon_2} \end{pmatrix}^T, \\
\Psi_2^*(s) &= \frac{q_1(s)-q_2(s)}{2i} = \begin{pmatrix} \mathrm{Im}\{e^{-i\omega_0\tau^*s}\} \\ \mathrm{Im}\{\varsigma e^{-i\omega_0\tau^*s}\} \end{pmatrix}^T = \begin{pmatrix} -\sin\omega_0\tau^*s \\ \frac{k\beta\omega_0\cos\omega_0\tau^*s - r(\eta+\varepsilon_2)\sin\omega_0\tau^*s}{k\beta r - k\beta\eta - k\beta\varepsilon_1 - r\eta - r\varepsilon_2} \end{pmatrix}^T,
\end{aligned}$$

for $s \in [0, 1]$. From (4.9), we can obtain (Ψ_1^*, Φ_1) and (Ψ_1^*, Φ_2). Noting that

$$(q_1, p_1) = (\Psi_1^*, \Phi_1) - (\Psi_2^*, \Phi_2) + i[(\Psi_1^*, \Phi_2) + (\Psi_2^*, \Phi_1)]$$

and

$$(q_1, p_1) = 1 + \xi\varsigma + \tau^*\beta\xi S^* e^{-i\omega_0\tau^*}(\varsigma - 1) := D^*.$$

Therefore, we have

$$\begin{aligned}
&(\Psi_1^*, \Phi_1) - (\Psi_2^*, \Phi_2) = \mathrm{Re}\{D^*\}, \\
&(\Psi_1^*, \Phi_2) + (\Psi_2^*, \Phi_1) = \mathrm{Im}\{D^*\}.
\end{aligned}$$

Now, we define $(\Psi^*, \Phi) = (\Psi_j^*, \Phi_k)$ $(j, k = 1, 2)$ and construct a new basis Ψ for Q by $\Psi = (\Psi_1, \Psi_2)^T = (\Psi^*, \Phi)^{-1}\Psi^*$. Obviously, (Ψ, Φ) is a second order identity matrix. In addition, define $f_0 = (\beta_0^1, \beta_0^2)^T$, where

$$\beta_0^1 = \begin{pmatrix} 1 \\ 0 \end{pmatrix}, \qquad \beta_0^2 = \begin{pmatrix} 0 \\ 1 \end{pmatrix}.$$

Let $c \cdot f_0$ be defined by

$$c \cdot f_0 = c_1\beta_0^1 + c_2\beta_0^2,$$

for $c = (c_1, c_2)^T$, $c_j \in R$ $(j = 1, 2)$.

Then the center space of linear equation (4.5) is given by $P_{CN}\mathcal{C}$, where

$$P_{CN}\varphi = \Phi(\Psi, \langle\varphi, f_0\rangle) \cdot f_0, \quad \varphi \in \mathcal{C} \tag{4.12}$$

and

$$\mathcal{C} = P_{CN}\mathcal{C} \oplus P_S\mathcal{C},$$

here $P_S\mathcal{C}$ denotes the complementary subspace of $P_{CN}\mathcal{C}$.

Let A_{τ^*} be defined by

$$A_{\tau^*}\varphi(\theta) = \dot{\varphi}(\theta) + X_0(\theta)[\tau^* D\Delta\varphi(0) + L(\tau^*)(\varphi(\theta) - \dot{\varphi}(0))], \quad \varphi \in B\mathcal{C},$$

where $X_0 : [-1, 0] \to B(X, X)$ is given by

$$X_0(\theta) = \begin{cases} 0, & -1 \le \theta < 0, \\ I, & \theta = 0. \end{cases} \tag{4.13}$$

Then A_{τ^*} is the infinitesimal generator induced by the solution of (4.5) and (4.1) can be rewritten as the following operator differential equation

$$\dot{U}_t = A_{\tau^*} U_t + X_0 F(U_t, \mu). \tag{4.14}$$

Using the decomposition $\mathcal{C} = P_{CN}\mathcal{C} \oplus P_S\mathcal{C}$ and (4.12), the solution of (4.1) can be rewritten as

$$U_t = \Phi \begin{pmatrix} x_1(t) \\ x_2(t) \end{pmatrix} \cdot f_0 + h(x_1, x_2, \mu), \tag{4.15}$$

where

$$\begin{pmatrix} x_1(t) \\ x_2(t) \end{pmatrix} = (\Psi, \langle U_t, f_0 \rangle), \tag{4.16}$$

and $h(x_1, x_2, \mu) \in P_sC$ with $h(0, 0, 0) = Dh(0, 0, 0) = 0$. In particular, the solution of (4.1) on the center manifold is given by

$$U_t^* = \Phi \begin{pmatrix} x_1(t) \\ x_2(t) \end{pmatrix} \cdot f_0 + h(x_1, x_2, 0). \tag{4.17}$$

Setting $z = x_1 - ix_2$ and noticing that $p_1 = \Phi_1 + i\Phi_2$, then (4.17) can be rewritten as

$$U_t^* = \frac{1}{2}\Phi \begin{pmatrix} z + \bar{z} \\ i(z - \bar{z}) \end{pmatrix} \cdot f_0 + w(z, \bar{z}) = \frac{1}{2}(p_1 z + \bar{p_1}\bar{z}) \cdot f_0 + W(z, \bar{z}),$$

where $W(z, \bar{z}) = h(\frac{z+\bar{z}}{2}, -\frac{z-\bar{z}}{2i}, 0)$. Moreover, by [31], z satisfies

$$\dot{z} = i\omega_0\tau^* z + g(z, \bar{z}), \tag{4.18}$$

where

$$g(z, \bar{z}) = (\Psi_1(0) - i\Psi_2(0))\langle F(U_t^*, 0), f_0 \rangle. \tag{4.19}$$

Let

$$W(z, \bar{z}) = W_{20}\frac{z^2}{2} + W_{11} z\bar{z} + W_{02}\frac{\bar{z}^2}{2} + \cdots \tag{4.20}$$

and

$$g(z, \bar{z}) = g_{20}\frac{z^2}{2} + g_{11} z\bar{z} + g_{02}\frac{\bar{z}^2}{2} + \cdots. \tag{4.21}$$

From (4.17), we have

$$\begin{aligned} \langle F(U_t^*, 0), f_0 \rangle = {} & \frac{\tau^*}{4}\begin{pmatrix} \left(\frac{r}{k} - \beta\xi e^{-i\omega_0\tau^*}\right) z^2 + \left(-\frac{2r}{k} - \beta\bar{\xi} e i\omega_0\tau^* - \beta\xi e - i\omega_0\tau^*\right) z\bar{z} + \left(-\frac{r}{k} - \beta\bar{\xi} e^{i\omega_0\tau^*}\right)\bar{z}^2 \\ \beta\xi e^{-i\omega_0\tau^*} z^2 + (\beta\bar{\xi} e^{i\omega_0\tau^*} + \beta\xi e^{-i\omega_0\tau^*}) z\bar{z} + \beta\bar{\xi} e^{i\omega_0\tau^*}\bar{z}^2 \end{pmatrix} \\ & + \frac{\tau^*}{4}\begin{pmatrix} \left\langle -\frac{r}{k}(2W_{20}^{(1)}(0) + 4W_{11}^{(1)}(0)) - \beta(2W_{11}^{(2)}(-1) + W_{20}^{(2)}(-1) + 2W_{11}^{(1)}(0)\xi e^{-i\omega_0\tau^*} + \bar{\xi} W_{20}^{(1)}(0) e^{i\omega_0\tau^*}), 1 \right\rangle \\ \langle \beta(2W_{11}^{(2)}(-1) + W_{20}^{(2)}(-1) + 2W_{11}^{(1)}(0)\xi e^{-i\omega_0\tau^*} + \bar{\xi} W_{20}^{(1)}(0) e^{i\omega_0\tau^*}), 1 \rangle \end{pmatrix} z^2\bar{z} + \cdots, \end{aligned}$$

where

$$\langle W_{ij}^n(\theta), 1 \rangle = \frac{1}{\pi}\int_0^\pi W_{ij}^n(\theta)(x)dx, \quad i + j = 2, n \in \mathbb{N}.$$

Let $(\psi_1, \psi_2) = \Psi_1(0) - i\Psi_2(0)$. Then by (4.19)–(4.21), we can obtain the following quantities

$$\begin{aligned} g_{20} &= \frac{\tau^*}{2}\left[\left(-\frac{r}{k} - \beta\xi e^{-i\omega_0\tau^*}\right)\psi_1 + \beta\xi e^{-i\omega_0\tau^*}\psi_2\right], \\ g_{11} &= \frac{\tau^*}{4}\left[\left(-\frac{2r}{k} - \beta\bar{\xi} e^{i\omega_0\tau^*} - \beta\xi e^{-i\omega_0\tau^*}\right)\psi_1 + (\beta\bar{\xi} e^{i\omega_0\tau^*} + \beta\xi e^{-i\omega_0\tau^*})\psi_2\right], \\ g_{02} &= \frac{\tau^*}{2}\left[\left(-\frac{r}{k} - \beta\bar{\xi} e^{i\omega_0\tau^*}\right)\psi_1 + \beta\bar{\xi} e^{i\omega_0\tau^*}\psi_2\right], \\ g_{21} &= \frac{\tau^*}{2}\left[\left\langle -\frac{r}{k}(2W_{20}^{(1)}(0) + 4W_{11}^{(1)}(0)) - \beta(2W_{11}^{(2)}(-1) + W_{20}^{(2)}(-1) + 2W_{11}^{(1)}(0)\xi e^{-i\omega_0\tau^*} + \bar{\xi} W_{20}^{(1)}(0) e^{i\omega_0\tau^*}), 1 \right\rangle \psi_1 \right. \\ &\quad \left. + \langle \beta(2W_{11}^{(2)}(-1) + W_{20}^{(2)}(-1) + 2W_{11}^{(1)}(0)\xi e^{-i\omega_0\tau^*} + \bar{\xi} W_{20}^{(1)}(0) e^{i\omega_0\tau^*}), 1 \rangle \psi_2\right]. \end{aligned}$$

Since $W_{20}(\theta)$, $W_{11}(\theta)$ for $\theta \in [-1, 0]$ appear in g_{21}, we still need to compute them. It easily follows from (4.20) that

$$\dot{W}(z, \bar{z}) = W_{20} z\dot{z} + W_{11}(\dot{z}\bar{z} + z\dot{\bar{z}}) + W_{02}\bar{z}\dot{\bar{z}} + \cdots \tag{4.22}$$

and

$$A_{\tau^*} W = A_{\tau^*} W_{20} \frac{z^2}{2} + A_{\tau^*} W_{11} z\bar{z} + A_{\tau^*} W_{02} \frac{\bar{z}^2}{2} + \cdots. \tag{4.23}$$

In addition, by [31], $W(z(t), \bar{z}(t))$ satisfies

$$\dot{W} = A_{\tau^*} W + H(z, \bar{z}), \tag{4.24}$$

where

$$(z, \bar{z}) = H_{20} \frac{z^2}{2} + H_{11} z\bar{z} + H_{02} \frac{\bar{z}^2}{2} + \cdots = X_0 F(U_t^*, 0) - \Phi(\Psi, \langle X_0 F(U_t^*, 0), f_0\rangle) \cdot f_0,$$

with $H_{ij} \in P_S \mathcal{C}$, $i + j = 2$.

Thus, from (4.18) and (4.22)–(4.24), we can obtain that

$$\begin{cases} (2i\omega_0\tau^* - A_{\tau^*}) W_{20} = H_{20}, \\ -A_{\tau^*} W_{11} = H_{11}. \end{cases} \tag{4.25}$$

Noticing that A_{τ^*} has only two eigenvalues $\pm i\omega_0\tau^*$ with zero real parts, therefore, (4.24) has unique solution $W_{ij}(i+j = 2)$ in $P_S \mathcal{C}$ given by

$$\begin{cases} W_{20} = (2i\omega_0\tau^* - A_{\tau^*})^{-1} H_{20}, \\ W_{11} = -A_{\tau^*}^{-1} H_{11}. \end{cases} \tag{4.26}$$

From (4.25), we know that for $-1 \le \theta < 0$,

$$\begin{aligned} H(z, \bar{z}) &= -\Phi(\theta)\Psi(0)\langle F(U_t^*, 0), f_0\rangle \cdot f_0 \\ &= -\left(\frac{p_1(\theta) + p_2(\theta)}{2}, \frac{p_1(\theta) - p_2(\theta)}{2i}\right)(\Psi_1(0), \Psi_2(0))^T \times \langle F(U_t^*, 0), f_0\rangle \cdot f_0 \\ &= -\frac{1}{2}[p_1(\theta)(\Psi_1(0) - i\Psi_2(0)) + p_2(\theta)(\Psi_1(0) + i\Psi_2(0))] \times \langle F(U_t^*, 0), f_0\rangle \cdot f_0 \\ &= -\frac{1}{4}[g_{20} p_1(\theta) + \bar{g}_{02} p_2(\theta)] z^2 \cdot f_0 - \frac{1}{2}[g_{11} p_1(\theta) + \bar{g}_{11} p_2(\theta)] z\bar{z} \cdot f_0 + \cdots \end{aligned}$$

Therefore, for $-1 \le \theta < 0$,

$$H_{20}(\theta) = -\frac{1}{2}[g_{20} p_1(\theta) + \bar{g}_{02} p_2(\theta)] \cdot f_0, \tag{4.27}$$

$$H_{11}(\theta) = -\frac{1}{2}[g_{11} p_1(\theta) + \bar{g}_{11} p_2(\theta)] \cdot f_0 \tag{4.28}$$

and

$$\begin{aligned} &H(z, \bar{z})(0) = F(U_t^*, 0) - \Phi(\Psi, \langle F(U_t^*, 0), f_0\rangle) \cdot f_0, \\ &H_{20}(0) = \frac{\tau^*}{2}\begin{pmatrix} -\frac{r}{k} - \beta\xi e^{-i\omega_0\tau^*} \\ \beta\xi e^{-i\omega_0\tau^*} \end{pmatrix} - \frac{1}{2}[g_{20} p_1(0) + \bar{g}_{02} p_2(0)] \cdot f_0, \end{aligned} \tag{4.29}$$

$$H_{11}(0) = \frac{\tau^*}{4}\begin{pmatrix} -\frac{2r}{k} - \beta\bar{\xi} e^{i\omega_0\tau^*} - \beta\xi e^{-i\omega_0\tau^*} \\ \beta\bar{\xi} e^{i\omega_0\tau^*} + \beta\xi e^{-i\omega_0\tau^*} \end{pmatrix} - \frac{1}{2}[g_{11} p_1(0) + \bar{g}_{11} p_2(0)] \cdot f_0. \tag{4.30}$$

By the definition of A_{τ^*}, we get from (4.26) that

$$\dot{W}_{20}(\theta) = 2i\omega_0\tau^* W_{20}(\theta) + \frac{1}{2}[g_{20} p_1(\theta) + \bar{g}_{02} p_2(\theta)] \cdot f_0, \ -1 \le \theta < 0.$$

Noting that $p_1(\theta) = p_1(0) e^{i\omega_0\tau^*}$, $-1 \le \theta \le 0$. Hence

$$W_{20}(\theta) = \frac{i}{2}\left[\frac{g_{20}}{\omega_0\tau^*} p_1(\theta) + \frac{\bar{g}_{02}}{3\omega_0\tau^*} p_2(\theta)\right] \cdot f_0 + E e^{2i\omega_0\tau^*\theta} \tag{4.31}$$

and

$$E = W_{20}(0) - \frac{i}{2}\left[\frac{g_{20}}{\omega_0\tau^*}p_1(0) + \frac{\bar{g}_{02}}{3\omega_0\tau^*}p_2(0)\right]\cdot f_0. \tag{4.32}$$

Using the definition of A_{τ^*}, and combining (4.26) and (4.32), we get

$$\begin{aligned}
&2i\omega_0\tau^*\left[\frac{ig_{20}}{2\omega_0\tau^*}p_1(0)\cdot f_0 + \frac{i\bar{g}_{02}}{6\omega_0\tau^*}p_2(0)\cdot f_0 + E\right] - \tau^*D\Delta\left[\frac{ig_{20}}{2\omega_0\tau^*}p_1(0)\cdot f_0 + \frac{i\bar{g}_{02}}{6\omega_0\tau^*}p_2(0)\cdot f_0 + E\right]\\
&\quad - L(\tau^*)\left[\frac{ig_{20}}{2\omega_0\tau^*}p_1(\theta)\cdot f_0 + \frac{i\bar{g}_{02}}{6\omega_0\tau^*}p_2(\theta)\cdot f_0 + Ee^{2i\omega_0\tau^*\theta}\right]\\
&= \frac{\tau^*}{2}\begin{pmatrix} -\frac{r}{k} - \beta\xi e^{-i\omega_0\tau^*} \\ \beta\xi e^{-i\omega_0\tau^*}\end{pmatrix} - \frac{1}{2}[g_{20}p_1(0) + \bar{g}_{02}p_2(0)]\cdot f_0.
\end{aligned}$$

Notice that

$$\begin{cases}\tau^*D\Delta[p_1(0)\cdot f_0] + L(\tau^*)[p_1(\theta)\cdot f_0] = i\omega_0\tau^*p_1(0)\cdot f_0,\\ \tau^*D\Delta[p_2(0)\cdot f_0] + L(\tau^*)[p_2(\theta)\cdot f_0] = -i\omega_0\tau^*p_2(0)\cdot f_0.\end{cases}$$

Then

$$2i\omega_0\tau^*E - \tau^*D\Delta E - L(\tau^*)(Ee^{2i\omega_0\tau^*\theta}) = \frac{\tau^*}{2}\begin{pmatrix} -\frac{r}{k} - \beta\xi e^{-i\omega_0\tau^*} \\ \beta\xi e^{-i\omega_0\tau^*}\end{pmatrix}.$$

From the above expression, we can see easily that

$$E = \frac{1}{2}\begin{pmatrix} 2i\omega_0 + \eta + \varepsilon_1 + \frac{2S^*r}{k} & \beta S^* \\ -\beta I^* & 2i\omega_0 + \eta + \varepsilon_2 - \beta S^*\end{pmatrix}^{-1} \times \begin{pmatrix} -\frac{r}{k} - \beta\xi e^{-i\omega_0\tau^*} \\ \beta\xi e^{-i\omega_0\tau^*}\end{pmatrix}.$$

In the similar way, we have

$$\dot{W}_{11}(\theta) = \frac{1}{2}[g_{11}p_1(\theta) + \bar{g}_{11}p_2(\theta)]\cdot f_0, \quad -1 \le \theta < 0$$

and

$$W_{11}(\theta) = \frac{i}{2\omega_0\tau^*}[-g_{11}p_1(\theta) + \bar{g}_{11}p_2(\theta)]\cdot f_0 + F.$$

Similar to the above, we can obtain that

$$F = \frac{1}{4}\begin{pmatrix} \eta + \varepsilon_1 + \frac{2S^*r}{k} + \beta I^* - r & \beta S^* \\ -\beta I^* & \eta + \varepsilon_2 - \beta S^*\end{pmatrix}^{-1} \times \begin{pmatrix} -\frac{2r}{k} - \beta\bar{\xi}e^{i\omega_0\tau^*} - \beta\xi e^{-i\omega_0\tau^*} \\ \beta\bar{\xi}e^{i\omega_0\tau^*} + \beta\xi e^{-i\omega_0\tau^*}\end{pmatrix}.$$

So far, $W_{20}(\theta)$ and $W_{11}(\theta)$ have been expressed by the parameters of system (3.1), Therefore, g_{21} can be expressed explicitly.

Theorem 3. *System (3.1) have the following Poincaré normal form*

$$\dot{\varrho} = i\omega_0\tau^*\varrho + c_1(0)\varrho|\varrho|^2 + o(|\varrho|^5),$$

where

$$c_1(0) = \frac{i}{2\omega_0\tau^*}\left(g_{20}g_{11} - 2|g_{11}|^2 - \frac{|g_{02}|^2}{3}\right) + \frac{g_{21}}{2},$$

so we can compute the following result

$$\begin{aligned}
\sigma_2 &= -\frac{\mathrm{Re}(c_1(0))}{\mathrm{Re}(\lambda'(\tau^*))},\\
\beta_2 &= 2\mathrm{Re}(c_1(0)),\\
T_2 &= -\frac{\mathrm{Im}(c_1(0)) + \sigma_2\mathrm{Im}(\lambda'(\tau^*))}{\omega_0\tau^*},
\end{aligned}$$

which determine the properties of bifurcating periodic solutions at the critical values τ^*, i.e., σ_2 determines the directions of the Hopf bifurcation: if $\sigma_2 > 0$ ($\sigma_2 < 0$), then the Hopf bifurcation is supercritical (subcritical) and the bifurcating periodic solutions exist for $\tau > \tau^*$; β_2 determines the stability of the bifurcating periodic solutions: the bifurcating periodic solutions on the center manifold are stable (unstable), if $\beta_2 < 0$ ($\beta_2 > 0$); and T_2 determines the period of the bifurcating periodic solutions: the periodic increase(decrease), if $T_2 > 0$ ($T_2 < 0$).

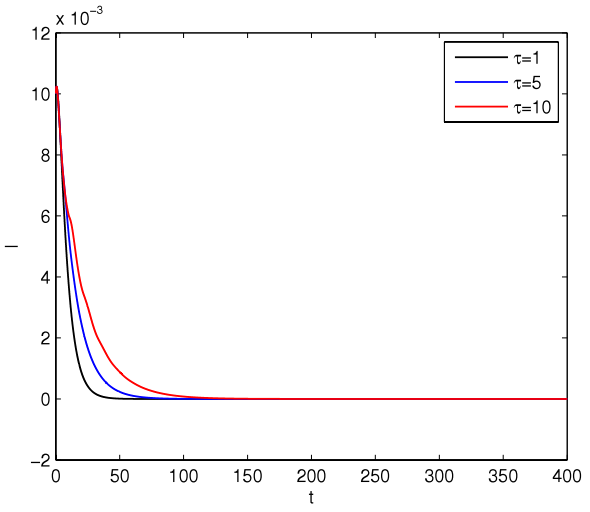

Fig. 1. The malware-free equilibrium point E^1 is locally asymptotically stable when $\tau = 1, 5, 10$.

5. Numerical simulation and discussion

In this section, we simulate and analyze the spatial–temporal dynamic characteristics of the proposed model through simulations on Matlab, including the trend in the quantity and spatial distribution of infected nodes.

5.1. Impact of delays on the density of infected nodes

To observe the impact of different delays on the density of the infected nodes, we consider system (1.4) with $\alpha = 0.4$, $\kappa = 7$, $r = 0.5$, $k = 0.9$, $\eta = 0.05$, $\varepsilon_1 = 0.2$, $\varepsilon_2 = 0.35$, $l = 1.25$, $d = 0.5$. By a simple calculation, it is easy to obtain that the malware-free equilibrium point E^1 is $(0.45, 0)^T$. Obviously, the conditions (H_1) and (H_3)–(H_4) hold. According to Theorem 1, system (1.4) is locally asymptotically stable for $\forall \tau \geq 0$. We assign 1, 5 and 10 to τ with the other parameters unchanged. The simulation results are shown in Fig. 1. From Fig. 1 we notice that the density of the infected nodes converges to the malware-free equilibrium point E^1 of system (1.4). Thus the malware propagation disappears. The simulation results in Fig. 1 verify Theorem 1. In addition, from Fig. 1 we notice that a larger τ implies a longer convergence time. This means a smaller τ can accelerate the process of malware extinction.

On the other hand, choose $\alpha = 0.3$, $\kappa = 7$, $r = 0.5$, $k = 0.96$, $\eta = 0.01$, $\varepsilon_1 = 0.05$, $\varepsilon_2 = 0.07$, $l = 1.4$, $d = 0.5$. It is easy to obtain that the positive equilibrium point of system (1.4) is $E^* = (0.1397, 0.6414)^T$. By calculating, the parameters satisfy the conditions of Theorem 2. According to Theorem 2, we can get the critical value is $\tau_0^0 = 3.4335$. We assign $1, 2, 3(< \tau_0^0)$ to τ with the other parameters unchanged. The simulation results are shown in Fig. 2(a). From Fig. 2(a), we notice that the density of infected nodes converges to the positive equilibrium point E^* of system (1.4). Thus the malware continuously propagates in MWSNs. The simulation results in Fig. 2(a) verify Theorem 2. In addition, from Fig. 2(a) we notice that a larger τ implies a longer convergence time. Next, we assign $4, 5, 6(> \tau_0^0)$ to τ with the other parameters unchanged. According to Theorem 2, the spatially homogeneous periodic solutions emerge from the positive equilibrium point E^*, as shown in Fig. 2(b). From Fig. 2(b), we notice that the malware propagation in MWSNs goes into periodic oscillation. In addition, from Fig. 2(b) we notice that a larger τ implies a larger oscillation period of the malware propagation. This means that when $\tau > \tau_0^0$, the delay enhances the degree of oscillation of the malware propagation. The above observations provide new insights into the malware propagation in MWSNs that the impact of delays on the density of infected nodes cannot be ignored, namely, with the delay τ increasing the mobile wireless sensor networks lose the stability through a Hopf bifurcation and some oscillations occur, which possibly leads to that the utilization of the networks decreases and the networks performance declines.

When $\tau = \tau_0^0 = 3.4335$, we can compute $c_1(0) = 0.1479 - 4.8493i$, $\sigma_2 = -\frac{0.1497}{\mathrm{Re}(\lambda'(\tau^*))} = -26.3801 < 0$, $\beta_2 = 2\mathrm{Re}(c_1(0)) = 0.2959 > 0$. Therefore, from the discussions in Section 4, we know that the bifurcating periodic solutions are orbitally unstable on the center manifold. In addition, from Theorem 3, we know that system (1.4) has an unstable center manifold near the positive equilibrium point E^* for τ near $\tau_0^0 = 3.4335$. Therefore, the center manifold theory implies that the bifurcating periodic solutions of system (1.4) when $\tau_0^0 = 3.4335$ in the whole phase space are orbitally unstable, and the Hopf bifurcation is subcritical for $\sigma_2 < 0$.

Remark 5.1.1. Keep the parameters $\alpha = 0.3$, $\kappa = 7$, $r = 0.5$, $k = 0.96$, $\eta = 0.01$, $\varepsilon_1 = 0.05$, $\varepsilon_2 = 0.07$, $l = 1.4$, $d = 0.5$. In this part, we discuss the effect of delay τ on the amplitude of the density of infected nodes when τ varies from 0 to 8 continuously. Fig. 3 gives the amplitude of the density of infected nodes for system (1.4) when $\tau \in [0, 8]$. From it we can

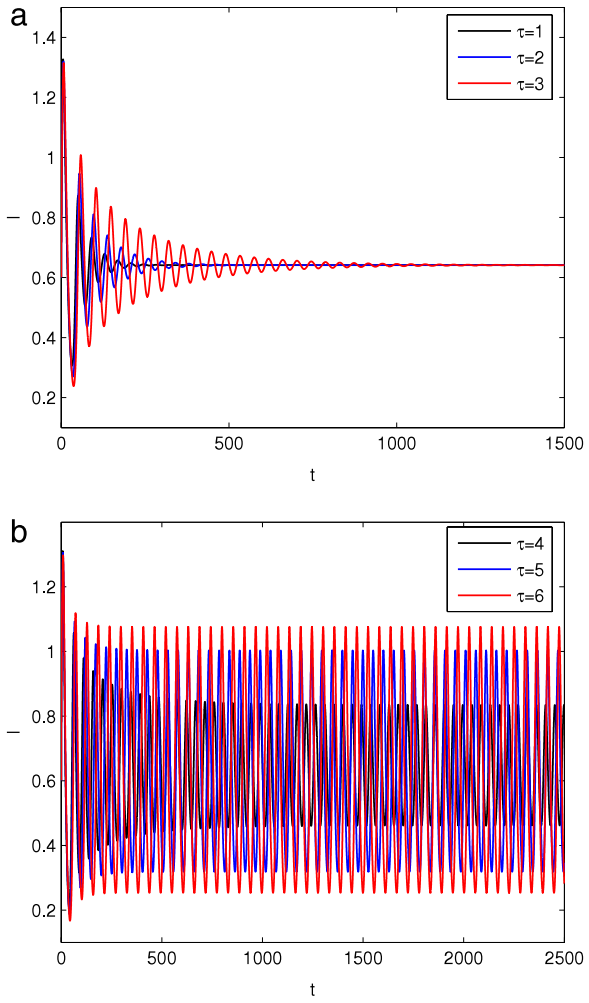

Fig. 2. Impact of delays on the density of infected nodes. (a) The positive equilibrium point E^* is stable when $\tau = 1, 2, 3 < \tau_0^0$; (b) Hopf bifurcation occurs from the positive equilibrium point E^* when $\tau = 4, 5, 6 > \tau_0^0$.

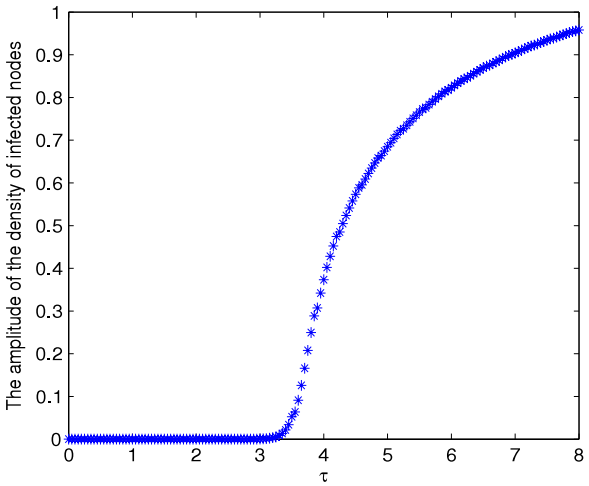

Fig. 3. The amplitude of the density of infected nodes varies with delay τ increasing.

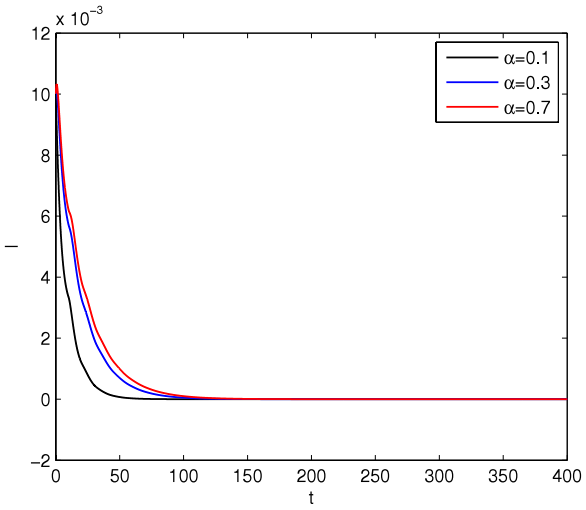

Fig. 4. The malware-free equilibrium point E^1 is locally asymptotically stable with α increasing when $\tau = 10$.

Table 1
The dynamic behavior of system (1.4) for different packet transmission rate α of wireless malware.

α	The equilibrium point	τ_0^0	$c_1(0)$	σ_2	β_2	T_2
0.3	$(0.1397, 0.6414)^T$	3.4335	0.1479–4.8493i	−26.3801	0.2959	32.6754
0.4	$(0.1319, 0.6123)^T$	3.3626	0.4302–4.7432i	−69.3477	0.8605	28.9196
0.5	$(0.1292, 0.6021)^T$	3.2433	0.5258–4.7172i	−81.9801	1.0516	27.8242

find that when $\tau < 3.4$ the amplitude is zero, which means system (1.4) is locally asymptotically stable at the positive equilibrium point E^*. That is, the malware continuously propagates in MWSNs with a fixed density of infected nodes. When $3.4 < \tau \leq 8$, as τ increasing the amplitude will increase. That is, system (1.4) is unstable and occurs oscillation which possibly leads to that the utilization of the network decreases and the networks performance declines. Moreover, Fig. 3 validates the analysis results above as well as Fig. 2.

5.2. Impact of packet transmission rate on the density of infected nodes

To observe the impact of packet transmission rate on the density of infected nodes, we let $\kappa = 7$, $r = 0.5$, $k = 0.9$, $\eta = 0.05$, $\varepsilon_1 = 0.2$, $\varepsilon_2 = 0.35$, $l = 1.25$, $d = 0.5$, and assign 0.1, 0.3 and 0.7 to α, respectively. By a simple calculation, it follows that the malware-free equilibrium point E^1 is $(0.45, 0)^T$. Obviously, the conditions (H_1) and (H_3)–(H_4) hold. According to Theorem 1, system (1.4) is locally asymptotically stable for $\forall \tau \geq 0$. We choose $\tau = 10$ with the other parameters unchanged. The simulation results are shown in Fig. 4. From Fig. 4 we notice that the density of the infected nodes converges to the malware-free equilibrium point E^1 of system (1.4). Thus the malware propagation disappears. The simulation results in Fig. 4 verify Theorem 1. In addition, from Fig. 4 we notice that a larger α implies a longer convergence time. This means that the process of malware will be more difficult to extinct with the packet transmission rate increasing.

On the other hand, choose $\kappa = 7$, $r = 0.5$, $k = 0.96$, $\eta = 0.01$, $\varepsilon_1 = 0.05$, $\varepsilon_2 = 0.07$, $l = 1.4$, $d = 0.5$, and assign 0.3, 0.4 and 0.5 to α, respectively. Obviously, the conditions (H_2) and (H_5)–(H_7) hold. According to Theorems 2 and 3, by calculating, it is easy to obtain the corresponding positive equilibrium points and the dynamic behavior of system (1.4) for different α, as shown in Table 1.

From Table 1, we can obtain that with the increasing of the packet transmission rate, the density of infected nodes and the critical value of τ decrease together. This means the malware propagation is sensitive to the packet transmission rate of nodes. Moreover, when $\tau = \tau_0^0$, we have $\sigma_2 < 0$, $\beta_2 > 0$. Therefore, from the discussions in Section 4, we know that the bifurcating periodic solutions are orbitally unstable on the center manifold. In addition, from Theorem 3, we know that system (1.4) has an unstable center manifold near the positive equilibrium point E^* for τ near τ_0^0. Therefore, the spatially homogeneous bifurcating periodic solution are unstable on the center manifold and the Hopf bifurcation is subcritical. We cannot get the bifurcating periodic solutions from simulations [33].

Without loss of generality, we assign $\tau = 1 < \tau_0^0$ with the other parameters unchanged. The simulation results are shown in Fig. 5(a). From Fig. 5(a), we notice that the density of infected nodes converges to the positive equilibrium point E^* of system (1.4). Thus the malware continuously propagates in MWSNs. The simulation results in Fig. 5(a) verify Theorem 2. In addition, from Fig. 5(a) we notice that a larger α implies a longer convergence time and at last the density of infected nodes decreases with the increasing of the packet transmission rate. When $\tau = 4 > \tau_0^0$, according to Theorem 2, the spatially homogeneous periodic solutions emerge from the positive equilibrium point E^*, as shown in Fig. 5(b). From Fig. 5(b),

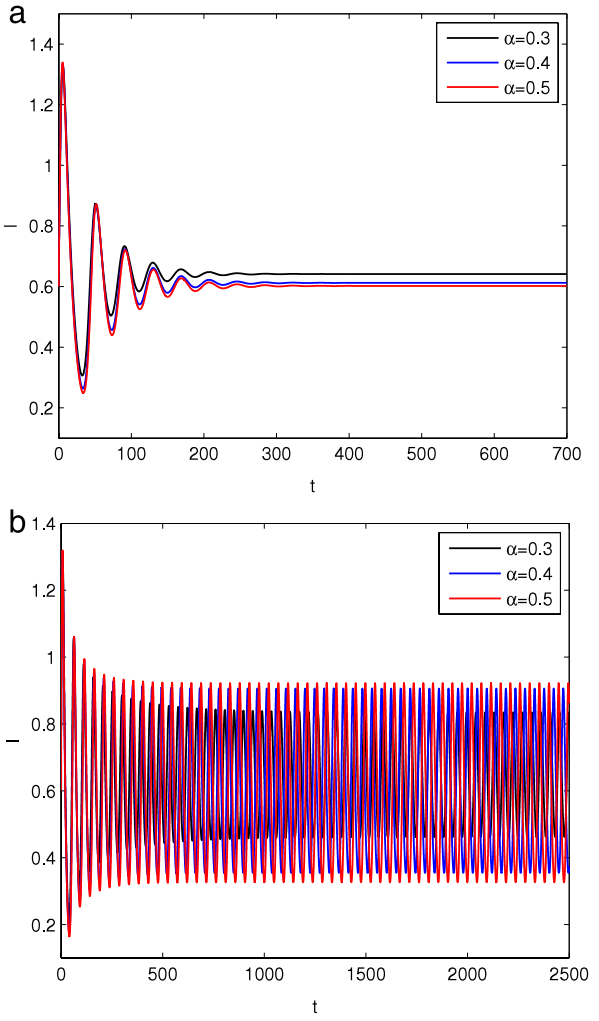

Fig. 5. Impact of packet transmission rate on the density of infected nodes. (a) The positive equilibrium point E^* is stable with α increasing when $\tau = 1 < \tau_0^0$; (b) Hopf bifurcation occurs from the positive equilibrium point E^* with α increasing when $\tau = 4 > \tau_0^0$.

we notice that the malware propagation in MWSNs goes into periodic oscillation. In addition, from Fig. 5(b) we notice that a larger α implies a larger oscillation period of the malware propagation. This means that when $\tau > \tau_0^0$, the packet transmission rate of nodes enhances the degree of oscillation of the malware propagation, which possibly leads to that the utilization of the networks decreases and the networks performance declines.

Remark 5.2.1. Keep the parameters $\kappa = 7, r = 0.5, k = 0.96, \eta = 0.01, \varepsilon_1 = 0.05, \varepsilon_2 = 0.07, l = 1.4, d = 0.5$. In this part, we discuss the effect of packet transmission rate α of wireless malware on the region of stability of system (1.4) when α varies from 0 to 1 continuously, as shown in Fig. 6. When $0 < \alpha < 0.1$, the region of stability of system (1.4) quickly becomes larger and we can see even though $\tau = 35$, system (1.4) is also locally asymptotically stable. When $0.1 \leq \alpha \leq 1$, it is easy to show that the region of stability of system (1.4) quickly becomes smaller and at last if we choose $\tau = 4$, system (1.4) will occur oscillation. The above observations provide new insight into the malware propagation in MWSNs. Moreover, Fig. 6 validates the numerical results above.

Remark 5.2.2. Keep the parameters $\kappa = 7, r = 0.5, k = 0.96, \eta = 0.01, \varepsilon_1 = 0.05, \varepsilon_2 = 0.07, l = 1.4, d = 0.5$ and let $\tau = 4$. In this part, we discuss the effect of packet transmission rate α of wireless malware on the amplitude of system (1.4) when α varies from 0 to 1 continuously. Fig. 7 gives the amplitude of the density of infected nodes when $\alpha \in [0, 1]$. From it we can find that when $\tau < 0.2$ the amplitude is zero, which means the system (1.4) is locally asymptotically stable at the positive equilibrium point E^*. That is, the malware continuously propagates in MWSNs with a fixed density of infected nodes. When $0.2 < \alpha \leq 1$, as α increasing the amplitude will increase and at last the amplitude arrives to a relatively fixed value. That is, system (1.4) is unstable and occurs oscillation which possibly leads to that the utilization of the networks decreases and the networks performance declines. Moreover, Fig. 7 validates the analysis results above as well as Fig. 5(b).

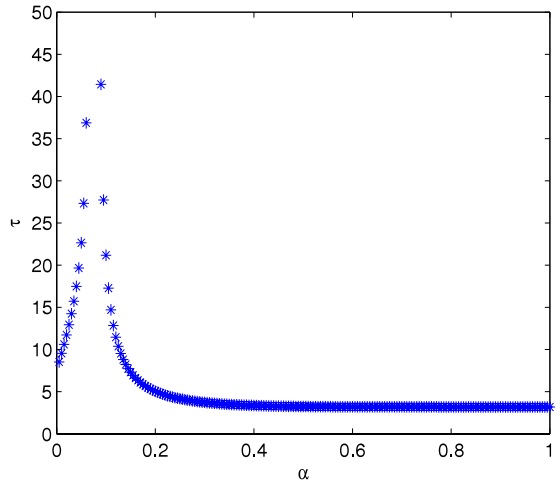

Fig. 6. The region of stability of system (1.4) varies with the packet transmission rate α increasing.

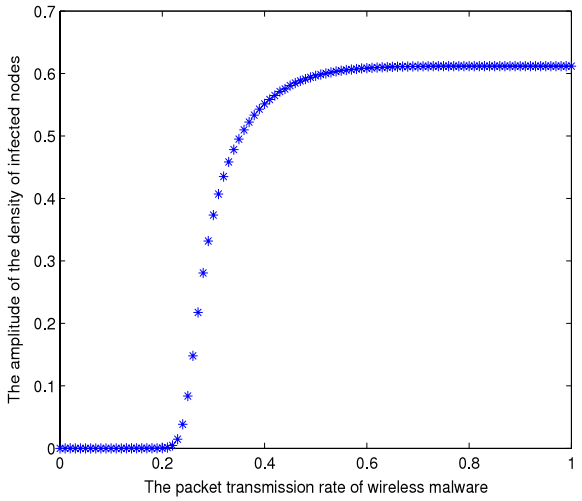

Fig. 7. The amplitude of the density of infected nodes varies with the packet transmission rate α increasing.

The above observations demonstrate that the packet transmission rate α of wireless malware is sensitive to the malware propagation in MWSNs.

5.3. Impact of communication radius on the density of infected nodes

To observe the impact of communication radius on the density of infected nodes, we let $\alpha = 0.4, \kappa = 7, r = 0.5, k = 0.9, \eta = 0.05, \varepsilon_1 = 0.2, \varepsilon_2 = 0.35, d = 0.5$, and assign 0.25, 0.85, and 1.45 to l, respectively. By a simple calculation, it is easy to show that the malware-free equilibrium point E^1 is $(0.45, 0)^T$. Obviously, the conditions (H_1) and (H_3)–(H_4) satisfy. According to Theorem 1, system (1.4) is locally asymptotically stable for $\forall \tau \geq 0$. We choose $\tau = 5$ with the other parameters unchanged. The simulation results are shown in Fig. 8. From Fig. 8 we notice that the density of the infected nodes converges to the malware-free equilibrium point E^1 of system (1.4). Thus the malware propagation disappears in MWSNs. In addition, from Fig. 8 we notice that a larger l implies a longer extinction process.

On the other hand, choose $\alpha = 0.3, \kappa = 7, r = 0.5, k = 0.96, \eta = 0.01, \varepsilon_1 = 0.05, \varepsilon_2 = 0.07, d = 0.5$, and assign 1.2, 1.3 and 1.4 to l, respectively. Obviously, the conditions (H_2) and (H_5)–(H_7) hold. According to Theorems 2 and 3, by calculating, it is easy to obtain the corresponding positive equilibrium points and the dynamic behavior of system (1.4) for different l, as shown in Table 2.

From Table 2, we can obtain that with the increasing of the communication radius, the critical value of τ decreases. This means that the region of stability of system (1.4) decreases and the malware propagation is sensitive to the communication radius of nodes. Moreover, if $l = 1.2$ or $l = 1.3$, then when $\tau = \tau_0^0$, we have $\sigma_2 > 0, \beta_2 < 0$. Therefore, from the discussions in Section 4, we know that the bifurcating periodic solutions are orbitally asymptotically stable on the center manifold. In

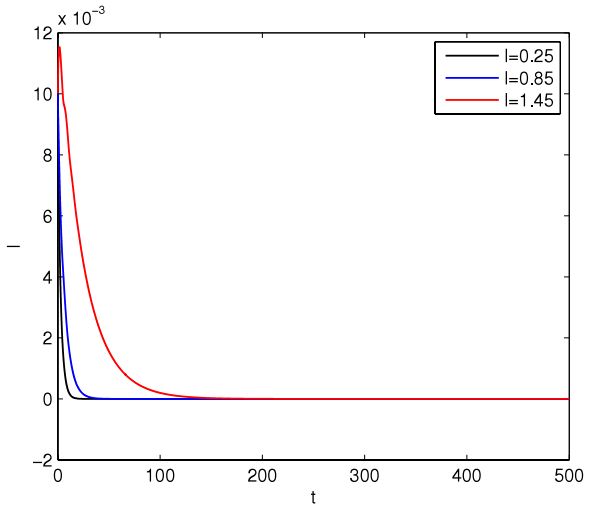

Fig. 8. The malware-free equilibrium point E^1 is locally asymptotically stable with l increasing when $\tau = 5$.

Table 2
The dynamic behavior of system (1.4) for different communication radius l of nodes.

l	The equilibrium point	τ_0^0	$c_1(0)$	σ_2	β_2	T_2
1.4	$(0.1397, 0.6414)^T$	3.4335	$0.1479-4.8493i$	−26.3801	0.2959	32.6754
1.3	$(0.1621, 0.7203)^T$	5.0330	$-5.4567-0.7564i$	187.6477	−1.5129	50.3982
1.2	$(0.1502, 0.8106)^T$	7.4715	$-7.2429-2.4166i$	1020.9641	−4.8332	105.8312

addition, from Theorem 3, we know that system (1.4) has a stable center manifold near the positive equilibrium point E^* for τ near τ_0^0. Therefore, the center manifold theory implies that the bifurcated periodic solutions of system (1.4) when $\tau = \tau_0^0$ in the whole phase space are orbitally asymptotically stable, and the Hopf bifurcation is supercritical for $\sigma_2 > 0$. And when $l = 1.4$, we have $\sigma_2 < 0, \beta_2 > 0$. Therefore, from the discussions in Section 4, we know that the bifurcating periodic solutions are orbitally unstable on the center manifold. In addition, from Theorem 3, we know that the system (1.4) has an unstable center manifold near the positive equilibrium point E^* for τ near τ_0^0. Therefore, the center manifold theory implies that the bifurcating periodic solutions of system (1.4) when $\tau = \tau_0^0$ in the whole phase space are unstable, and the Hopf bifurcation is subcritical for $\sigma_2 < 0$.

Then, we assign $\tau = 3 < \tau_0^0$ with the other parameters unchanged. The simulation results are shown in Fig. 9(a). From Fig. 9(a), we notice that the density of infected nodes converges to the positive equilibrium point E^* of system (1.4). Thus at last the malware continuously propagates in MWSNs. The simulation results in Fig. 9(a) verify Theorem 2. In addition, from Fig. 9(a) we notice that with the increasing of the communication radius, the convergence time is becoming longer and at last the density of infected nodes is decreasing. When $\tau = 7.9 > \tau_0^0$, according to Theorem 2, the spatially homogeneous periodic solutions emerge from the positive equilibrium point E^*, as shown in Fig. 9(b). From Fig. 9(b), we notice that the malware propagation in MWSNs goes into periodic oscillation. In addition, from Fig. 9(b) we notice that a larger l implies a larger oscillation period of the malware propagation. This means that when $\tau > \tau_0^0$, the communication radius of nodes enhances the degree of oscillation of the malware propagation, which possibly leads to that the utilization of the networks decreases and the networks performance declines.

Remark 5.3.1. Keep the parameters $\alpha = 0.3, \kappa = 7, r = 0.5, k = 0.96, \eta = 0.01, \varepsilon_1 = 0.05, \varepsilon_2 = 0.07, d = 0.5$. In this part, we discuss the effect of communication radius l of nodes on the region of stability of system (1.4) when l varies from 0 to 1.8 continuously, as shown in Fig. 10. When $0 < l < 1$, the region of stability of system (1.4) quickly becomes larger and we can see even though $\tau = 60$, system (1.4) is also locally asymptotically stable. When $1 \leq l \leq 1.8$, it is easy to show that the region of stability of system (1.4) quickly becomes smaller and at last the region of stability is close to zero. That is, if we choose $\tau = 4$ when $l = 1.4$, system (1.4) will occur oscillation, which possibly leads to that the network performance declines. Moreover, Fig. 10 validates the numerical results above.

Remark 5.3.2. Keep the parameters $\alpha = 0.3, \kappa = 7, r = 0.5, k = 0.96, \eta = 0.01, \varepsilon_1 = 0.05, \varepsilon_2 = 0.07, d = 0.5$ and let $\tau = 7.9$. In this part, we discuss the effect of communication radius l of nodes on the amplitude of system (1.4) when l varies from 0 to 2 continuously. Fig. 11 gives the amplitude of the density of infected nodes when $l \in [0, 2]$. From Fig. 11 we can find that when $l < 1.15$ the amplitude is zero, which means the system (1.4) is locally asymptotically stable at the positive equilibrium point E^*. That is, the malware continuously propagates in MWSNs with a fixed density of infected nodes. When

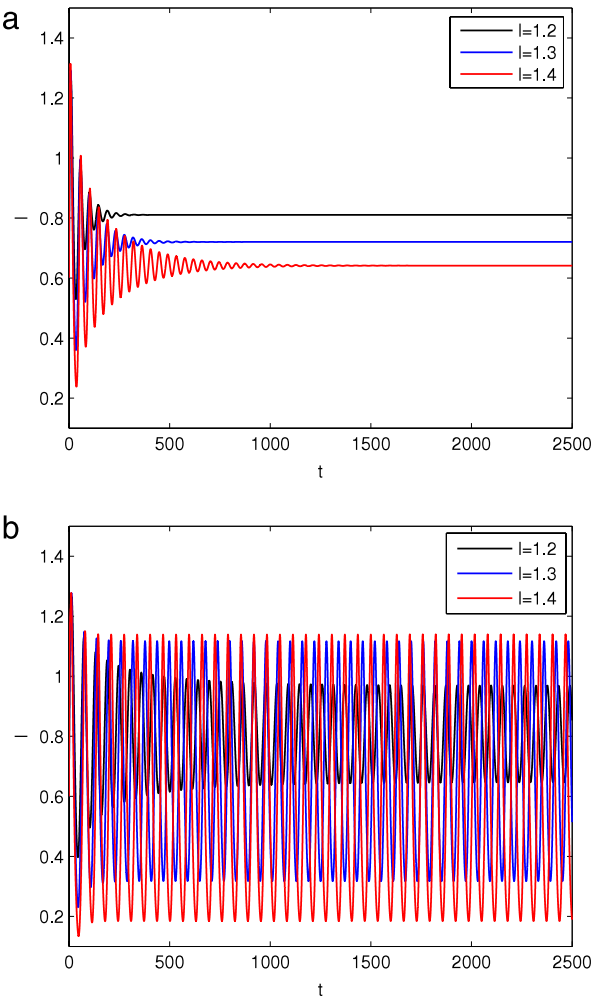

Fig. 9. Impact of communication radius on the density of infected nodes. (a) The positive equilibrium point E^* is stable with l increasing when $\tau = 3 < \tau_0^0$; (b) Hopf bifurcation occurs from the positive equilibrium point E^* with l increasing when $\tau = 7.9 > \tau_0^0$.

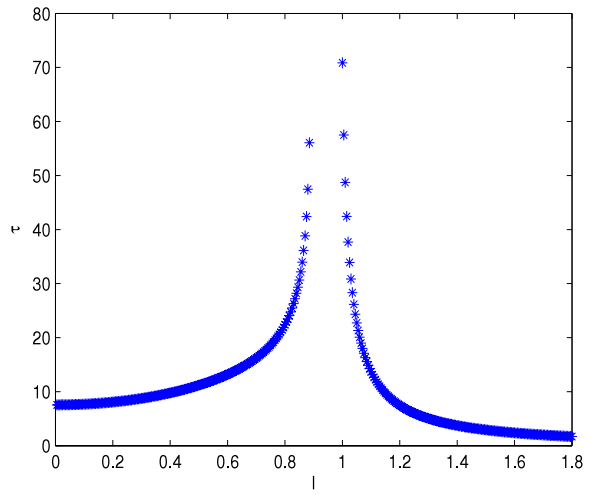

Fig. 10. The region of stability of system (1.4) varies with the communication radius l of nodes increasing.

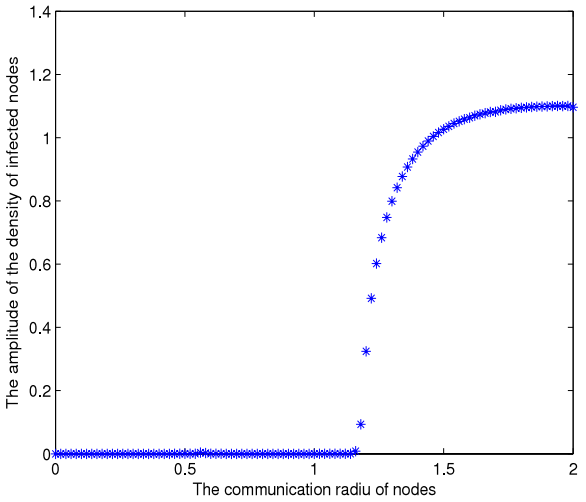

Fig. 11. The amplitude of the density of infected nodes varies with the communication radius l of nodes increasing.

$1.15 < l \leq 2$, as l increasing the amplitude will increase and at last the amplitude arrives to a relatively fixed value. That is, system (1.4) is unstable and occurs oscillation which possibly lead to that the utilization of the networks decreases and the networks performance declines. Moreover, Fig. 11 validates the analysis results above as well as Fig. 9(b). The above observations demonstrate that the communication radius l of nodes is sensitive to the malware propagation in MWSNs.

5.4. Impact of diffusion on the density of infected nodes

To observe the impact of diffusion coefficient on the density of infected nodes, we let $\alpha = 0.3, \kappa = 7, r = 0.5, k = 0.96, \eta = 0.01, \varepsilon_1 = 0.05, \varepsilon_2 = 0.07, l = 1.4$, and assign 0 and 1 to d, respectively. Obviously, the conditions (H_2) and (H_5)–(H_7) hold. According to Theorem 2, it follows that the positive equilibrium point E^* is $(0.1397, 0.6414)^T$ and the critical value is $\tau_0^0 = 3.4335$. As Fig. 12(a) shown, system (1.4) is asymptotically stable at the positive equilibrium E^* for $\tau = 3 < \tau_0^0$. Thus the malware continuously propagates in MWSNs. In addition, we notice that when $d = 1$, the convergence time of system (1.4) is longer. This means that the mobility of nodes restrains the convergence of the malware propagation. When $\tau = 4 > \tau_0^0$, according to Theorem 2, the spatially homogeneous periodic solutions emerge from the positive equilibrium point E^*, as shown in Fig. 12(b). From Fig. 12(b), we notice that the malware propagation in MWSNs goes into periodic oscillation. In addition, from Fig. 12(b) we notice that when $d = 1$ (MWSNs) the amplitude of the density of infected nodes increases. In fact, by a simple calculation, it is easy to obtain that when $d = 0$ (WSNs) the oscillation of the malware propagation is 0.3561 and the oscillation increases to 0.3691 when $d = 1$ (MWSNs), which means the mobility of nodes enhances the degree of oscillation of the malware propagation. The above observations provide that the diffusion we incorporated into the system can effect the convergence speed and the amplitude of system (1.4).

6. Conclusion

In this paper, to a reaction–diffusion modeling of malware propagation in MWSNs, we introduce discrete time delay into the modeling for investigating the spatial–temporal dynamics of malware propagation in MWSNs. Applying the theorem of partial function differential equation, we present verifiable conditions for stability and Hopf bifurcation of the system. Numerical simulations reveal that the discrete delay is responsible for the stability switch of the model, and a Hopf bifurcation occurs as the delay increasing through a certain threshold. Moreover, through numerical simulations we obtain that the spatial–temporal dynamic characteristics of malware propagation in MWSNs are closely related to the packet transmission rate, the communication range and the mobile behavior of nodes. In particular, our proposed model with the discrete delay can effectively predict both the temporal dynamic behavior and the spatial distribution of malware propagation in MWSNs. Thus, the reaction–diffusion modeling with the discrete delay provides new insights into the malware propagation in MWSNs.

Acknowledgments

This research is partially supported by the National Natural Science Foundation of China (Nos. 61174155, 11032009, 61173094, 61373083), and Qing Lan Project to Jiangsu. At the same time, the authors would like to express their gratitude to the editor and the anonymous reviewers for their valuable comments and suggestions.

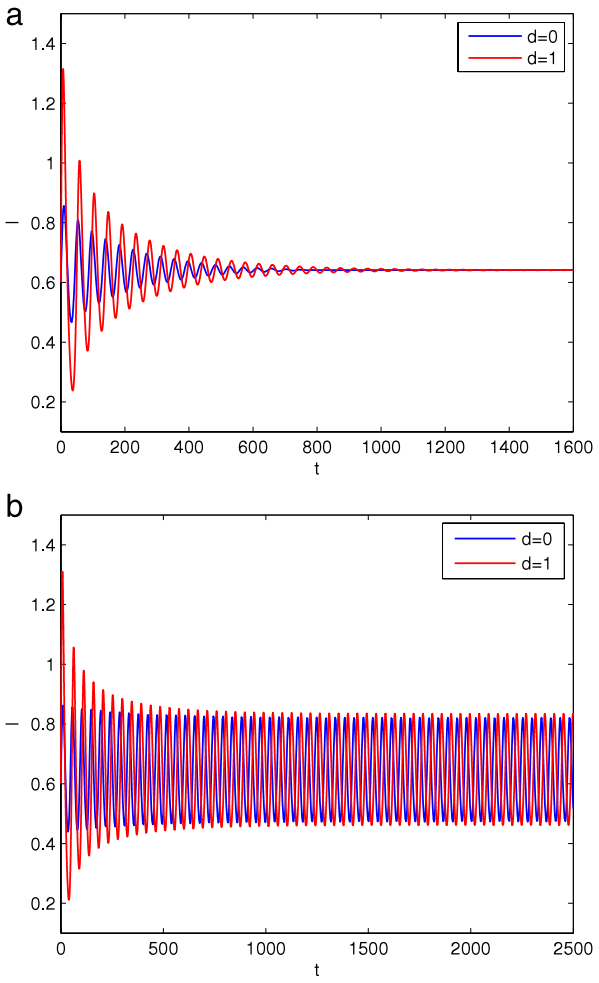

Fig. 12. Impact of diffusion coefficient on the density of infected nodes. (a) The positive equilibrium point E^* is stable with $d = 0$ and $d = 1$ when $\tau = 3 < \tau_0^0$; (b) Hopf bifurcation occurs from the positive equilibrium point E^* with $d = 0$ and $d = 1$ when $\tau = 4 > \tau_0^0$.

References

[1] D. Macedonio, M. Merro, A semantic analysis of key management protocols for wireless sensor networks, Sci. Comput. Program. 81 (2014) 53–78.
[2] M. Liu, H. Li, Y. Shen, J. Fan, S. Huang, Elastic neural network method for multi-target tracking task allocation in wireless sensor network, Comput. Math. Appl. 57 (11) (2009) 1822–1828.
[3] D.W. Marsh, R.O. Baldwin, B.E. Mullins, R.F. Mills, M.R. Grimaila, A security policy language for wireless sensor networks, J. Syst. Softw. 82 (1) (2009) 101–111.
[4] I.F. Akyildiz, W. Su, Y. Sankarasubramaniam, E. Cayirci, Wireless sensor networks: a survey, Comput. Netw. 38 (4) (2002) 393–422.
[5] J. Hu, L. Xie, C. Zhang, Energy-based multiple target localization and pursuit in mobile sensor networks, IEEE Trans. Instrum. Meas. 61 (1) (2012) 212–220.
[6] S. Ehsan, K. Bradford, M. Brugger, B. Hamdaoui, Y. Kovchegov, D. Johnson, M. Louhaichi, Design and analysis of delay-tolerant sensor networks for monitoring and tracking free-roaming animals, IEEE Trans. Wirel. Commun. 11 (3) (2012) 1220–1227.
[7] A. Boukerche, Y. Ren, A secure mobile healthcare system using trust-based multicast scheme, IEEE J. Sel. Areas Commun. 27 (4) (2009) 387–399.
[8] G. Tuna, V.C. Gungor, K. Gulez, An autonomous wireless sensor network deployment system using mobile robots for human existence detection in case of disasters, Ad Hoc Netw. 13 (2014) 54–68.
[9] M.I. Khan, W.N. Gansterer, G. Haring, Static vs. mobile sink: the influence of basic parameters on energy efficiency in wireless sensor networks, Comput. Commun. 36 (9) (2013) 965–978.
[10] A. Rasheed, R.N. Mahapatra, The three-tier security scheme in wireless sensor networks with mobile sinks, IEEE Trans. Parallel Distrib. Syst. 23 (5) (2012) 958–965.
[11] S. Peng, S. Li, X. Liao, Y. Peng, N. Xiao, A scalable code dissemination protocol in heterogeneous wireless sensor networks, Sci. China Inf. Sci. 55 (6) (2012) 1323–1336.
[12] I. Khalil, M. Awad, A. Khreishah, Ctac: control traffic tunneling attacks countermeasures in mobile wireless networks, Comput. Netw. 56 (14) (2012) 3300–3317.
[13] M. Khouzani, S. Sarkar, Maximum damage battery depletion attack in mobile sensor networks, IEEE Trans. Automat. Control 56 (10) (2011) 2358–2368.
[14] Z. Hu, Z. Teng, L. Zhang, Stability and bifurcation analysis of a discrete predator–prey model with nonmonotonic functional response, Nonlinear Anal. RWA 12 (4) (2011) 2356–2377.
[15] H. Zhu, Y. Luo, M. Chen, Stability and hopf bifurcation of a hiv infection model with ctl-response delay, Comput. Math. Appl. 62 (8) (2011) 3091–3102.
[16] G. Guo, B. Li, X. Lin, Hopf bifurcation in spatially homogeneous and inhomogeneous autocatalysis models, Comput. Math. Appl. 67 (1) (2014) 151–163.
[17] M.E. Newman, Spread of epidemic disease on networks, Phys. Rev. E 66 (1) (2002) 016128.

[18] H.W. Hethcote, The mathematics of infectious diseases, SIAM Rev. 42 (4) (2000) 599–653.
[19] Z. Hu, Z. Teng, H. Jiang, Stability analysis in a class of discrete sirs epidemic models, Nonlinear Anal. RWA 13 (5) (2012) 2017–2033.
[20] R. Xu, Z. Ma, Z. Wang, Global stability of a delayed sirs epidemic model with saturation incidence and temporary immunity, Comput. Math. Appl. 59 (9) (2010) 3211–3221.
[21] X. Shi, J. Cui, X. Zhou, Stability and hopf bifurcation analysis of an eco-epidemic model with a stage structure, Nonlinear Anal. TMA 74 (4) (2011) 1088–1106.
[22] L. Nie, Z. Teng, A. Torres, Dynamic analysis of an sir epidemic model with state dependent pulse vaccination, Nonlinear Anal. RWA 13 (4) (2012) 1621–1629.
[23] X. Wang, Q. Li, Y. Li, Eisirs: a formal model to analyze the dynamics of worm propagation in wireless sensor networks, J. Comb. Optim. 20 (1) (2010) 47–62.
[24] W. Xiaoming, L. Yingshu, An improved sir model for analyzing the dynamics of worm propagation in wireless sensor networks, Chin. J. Electron. 18 (1) (2009) 8–12.
[25] X. Wang, Z. He, X. Zhao, C. Lin, Y. Pan, Z. Cai, Reaction–diffusion modeling of malware propagation in mobile wireless sensor networks, Sci. China Inf. Sci. 56 (9) (2013) 1–18.
[26] J. Ren, X. Yang, Q. Zhu, L.-X. Yang, C. Zhang, A novel computer virus model and its dynamics, Nonlinear Anal. RWA 13 (1) (2012) 376–384.
[27] J.-J. Wang, J.-Z. Zhang, Z. Jin, Analysis of an sir model with bilinear incidence rate, Nonlinear Anal. RWA 11 (4) (2010) 2390–2402.
[28] L. Li, G.-Q. Sun, Z. Jin, Bifurcation and chaos in an epidemic model with nonlinear incidence rates, Appl. Math. Comput. 216 (4) (2010) 1226–1234.
[29] X. Zhang, H. Zhao, Bifurcation and optimal harvesting of a diffusive predator–prey system with delays and interval biological parameters, J. Theoret. Biol. 363 (2014) 390–403.
[30] J. Wu, Theory and Applications of Partial Functional Differential Equations, Vol. 119, Springer, 1996.
[31] J.K. Hale, Functional Differential Equations, Springer, 1971.
[32] T. Faria, Normal forms and hopf bifurcation for partial differential equations with delays, Trans. Amer. Math. Soc. 352 (5) (2000) 2217–2238.
[33] W. Zuo, J. Wei, Stability and hopf bifurcation in a diffusive predator–prey system with delay effect, Nonlinear Anal. RWA 12 (4) (2011) 1998–2011.